Supplementary Material
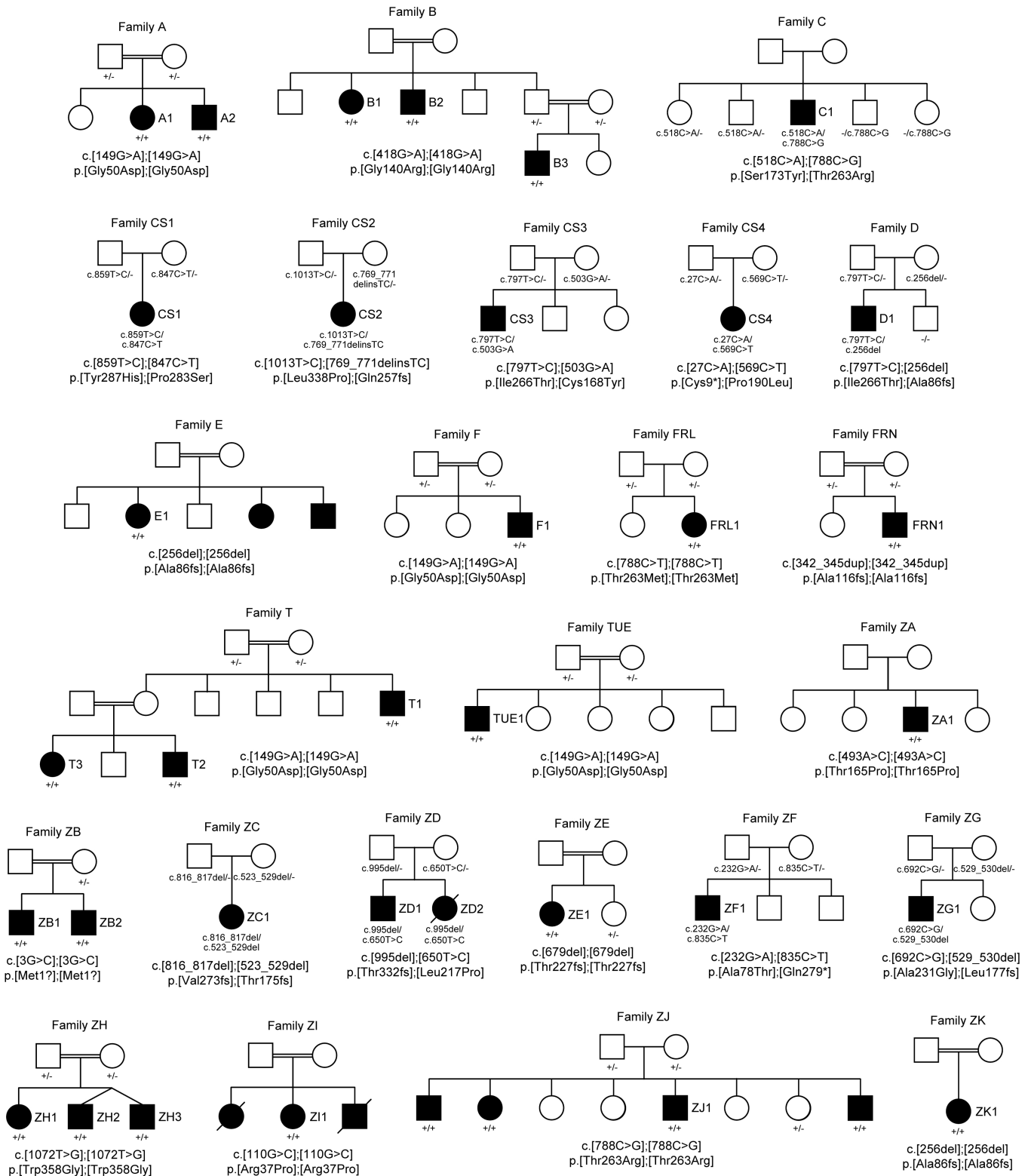

for

Wiessner *et al*.:

Biallelic variants in *HPDL* cause pure and complicated hereditary spastic paraplegia

Family A
+/- +/-
A1 A2
+/+ +/+
c.[149G>A];[149G>A]
p.[Gly50Asp];[Gly50Asp]

Family B
B1 B2 +/- +/-
+/+ +/+
B3
+/+
c.[418G>A];[418G>A]
p.[Gly140Arg];[Gly140Arg]

Family C
c.518C>A/- c.518C>A/- C1 -/c.788C>G -/c.788C>G
c.518C>A/
c.788C>G
c.[518C>A];[788C>G]
p.[Ser173Tyr];[Thr263Arg]

Family CS1
c.859T>C/- c.847C>T/-
CS1
c.859T>C/
c.847C>T
c.[859T>C];[847C>T]
p.[Tyr287His];[Pro283Ser]

Family CS2
c.1013T>C/- c.769_771
delinsTC/-
CS2
c.1013T>C/
c.769_771delinsTC
c.[1013T>C];[769_771delinsTC]
p.[Leu338Pro];[Gln257fs]

Family CS3
c.797T>C/- c.503G>A/-
CS3
c.797T>C/
c.503G>A
c.[797T>C];[503G>A]
p.[Ile266Thr];[Cys168Tyr]

Family CS4
c.27C>A/- c.569C>T/-
CS4
c.27C>A/
c.569C>T
c.[27C>A];[569C>T]
p.[Cys9*];[Pro190Leu]

Family D
c.797T>C/- c.256del/-
D1 -/-
c.797T>C/
c.256del
c.[797T>C];[256del]
p.[Ile266Thr];[Ala86fs]

Family E
E1
+/+
c.[256del];[256del]
p.[Ala86fs];[Ala86fs]

Family F
+/- +/-
F1
+/+
c.[149G>A];[149G>A]
p.[Gly50Asp];[Gly50Asp]

Family FRL
+/- +/-
FRL1
+/+
c.[788C>T];[788C>T]
p.[Thr263Met];[Thr263Met]

Family FRN
+/- +/-
FRN1
+/+
c.[342_345dup];[342_345dup]
p.[Ala116fs];[Ala116fs]

Family T
+/- +/-
T1
+/+
T3 T2
+/+ +/+
c.[149G>A];[149G>A]
p.[Gly50Asp];[Gly50Asp]

Family TUE
+/- +/-
TUE1
+/+
c.[149G>A];[149G>A]
p.[Gly50Asp];[Gly50Asp]

Family ZA
ZA1
+/+
c.[493A>C];[493A>C]
p.[Thr165Pro];[Thr165Pro]

Family ZB
+/-
ZB1 ZB2
+/+ +/+
c.[3G>C];[3G>C]
p.[Met1?];[Met1?]

Family ZC
c.816_817del/- c.523_529del/-
ZC1
c.816_817del/
c.523_529del
c.[816_817del];[523_529del]
p.[Val273fs];[Thr175fs]

Family ZD
c.995del/- c.650T>C/-
ZD1 ZD2
c.995del/ c.995del/
c.650T>C c.650T>C
c.[995del];[650T>C]
p.[Thr332fs];[Leu217Pro]

Family ZE
ZE1 +/-
c.[679del];[679del]
p.[Thr227fs];[Thr227fs]

Family ZF
c.232G>A/- c.835C>T/-
ZF1
c.232G>A/
c.835C>T
c.[232G>A];[835C>T]
p.[Ala78Thr];[Gln279*]

Family ZG
c.692C>G/- c.529_530del/-
ZG1
c.692C>G/
c.529_530del
c.[692C>G];[529_530del]
p.[Ala231Gly];[Leu177fs]

Family ZH
+/- +/-
ZH1 ZH2 ZH3
+/+ +/+ +/+
c.[1072T>G];[1072T>G]
p.[Trp358Gly];[Trp358Gly]

Family ZI
ZI1
+/+
c.[110G>C];[110G>C]
p.[Arg37Pro];[Arg37Pro]

Family ZJ
+/- +/-
ZJ1
+/+ +/+ +/+ +/- +/+
c.[788C>G];[788C>G]
p.[Thr263Arg];[Thr263Arg]

Family ZK
ZK1
+/+
c.[256del];[256del]
p.[Ala86fs];[Ala86fs]

**Supplementary Fig. 1** Pedigrees of HSP families with biallelic *HPDL* variants.

Squares represent males and circles represent females. Filled symbols correspond to affected and empty symbols correspond to unaffected subjects. *HPDL* genotypes of individuals from whom a DNA sample was available are given below the pedigree symbols. +/+ indicates homozygous for *HPDL* variant; +/- indicates heterozygous for *HPDL* variant; -/- indicates homozygous for wild-type *HPDL* sequence.
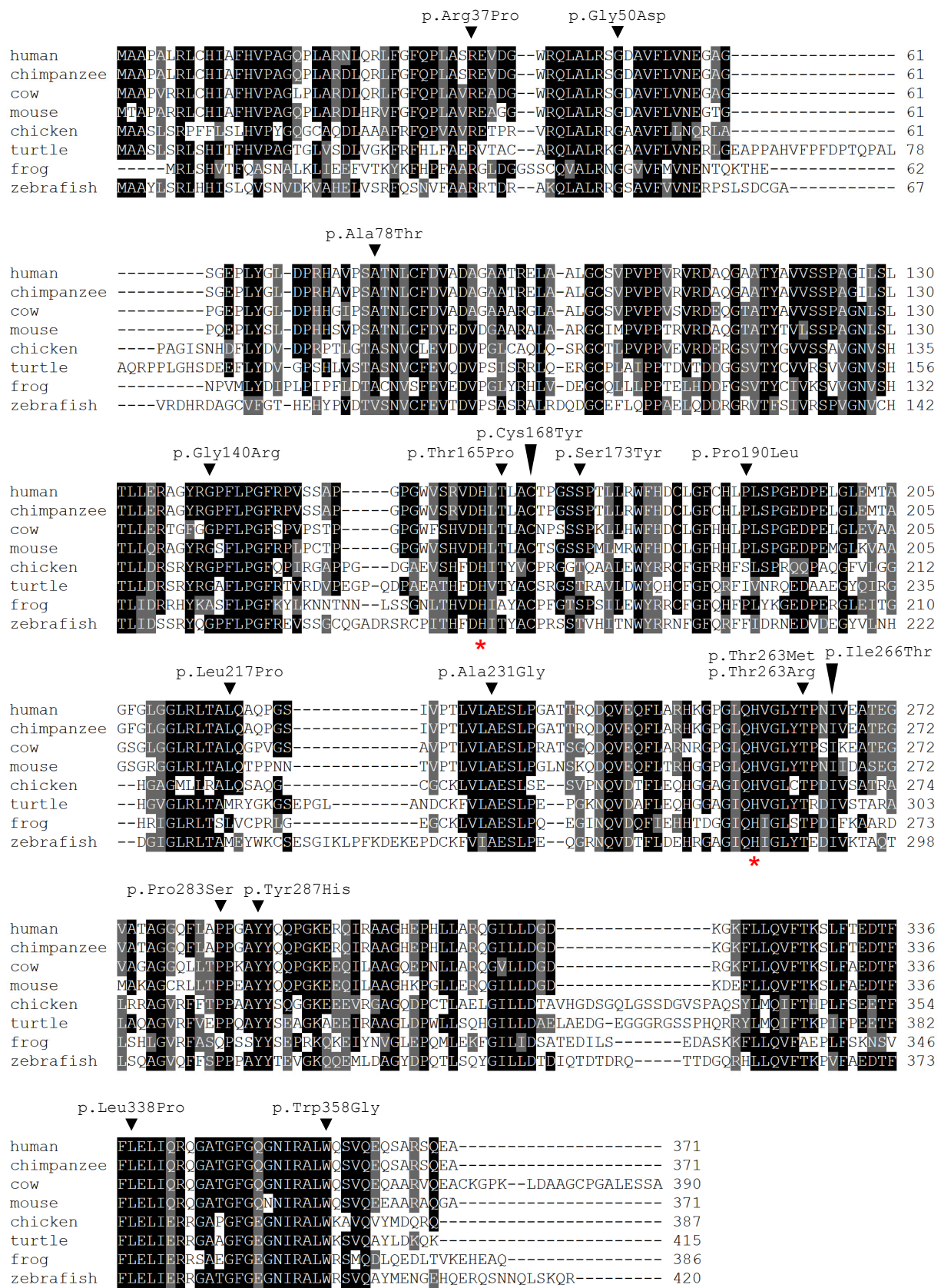
Supplementary Fig. 2 Multiple sequence alignment of human HPDL and its orthologs.

The alignment was generated with ClustalW (Larkin *et al.*, 2007) using UniProt or RefSeq sequences fof eight HPDLs (human: Q96IR7, chimpanzee: H2PYX0, cow: A5PJL0, mouse: Q8K248, chicken: E1BX51, turtle: XP_005303100.1, frog: B1WAT4, zebrafish: A7MC29).

HPDL missense variants (arrowheads) observed in subjects with HSP affect amino acids that are widely conserved or substituted conservatively across several species. Red asterisks indicate amino acids that coordinate the iron atom in the putative catalytic center of HPDL.
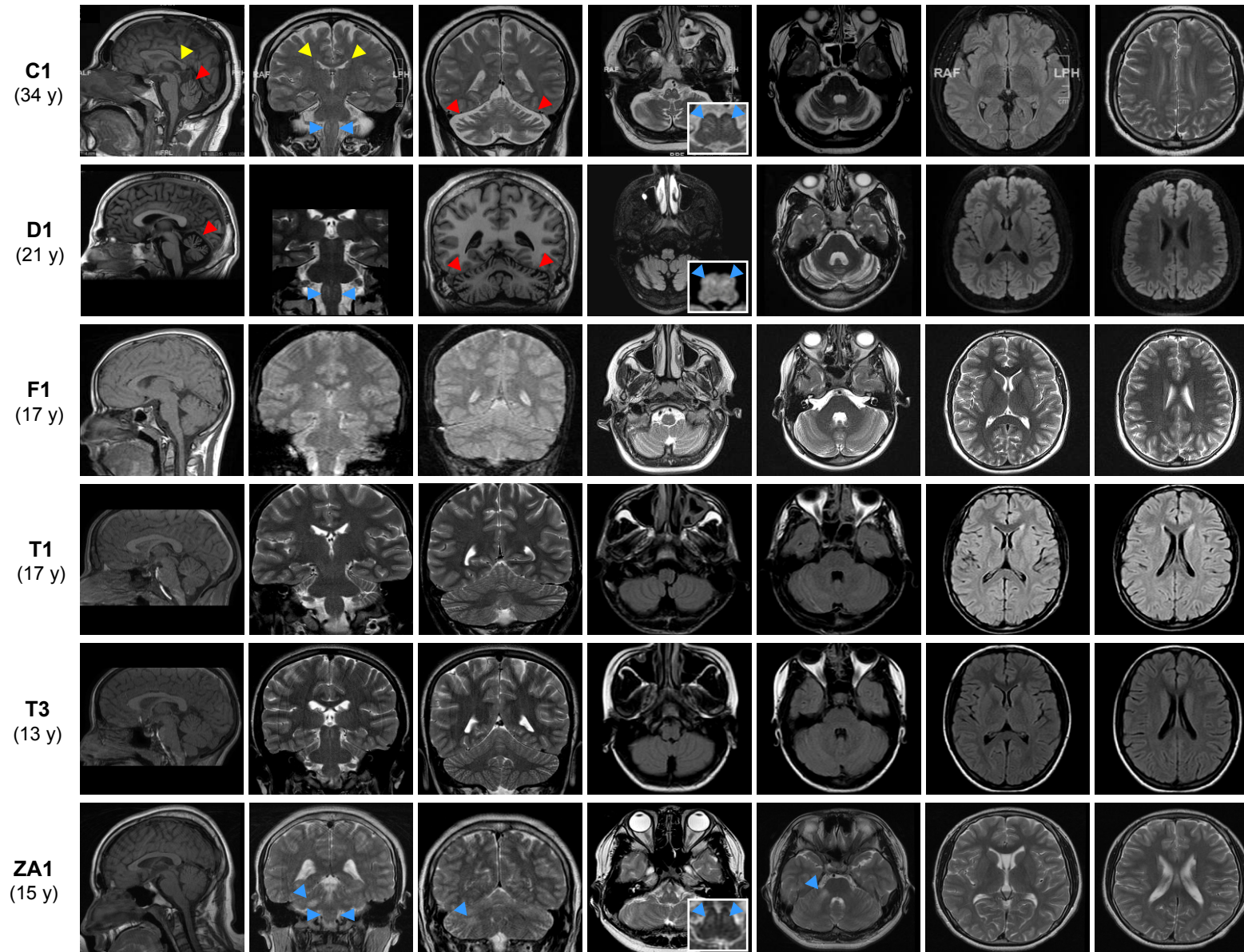
Supplementary Fig. 3 Neuroimaging in subjects with biallelic *HPDL* variants (*continued on next page*).
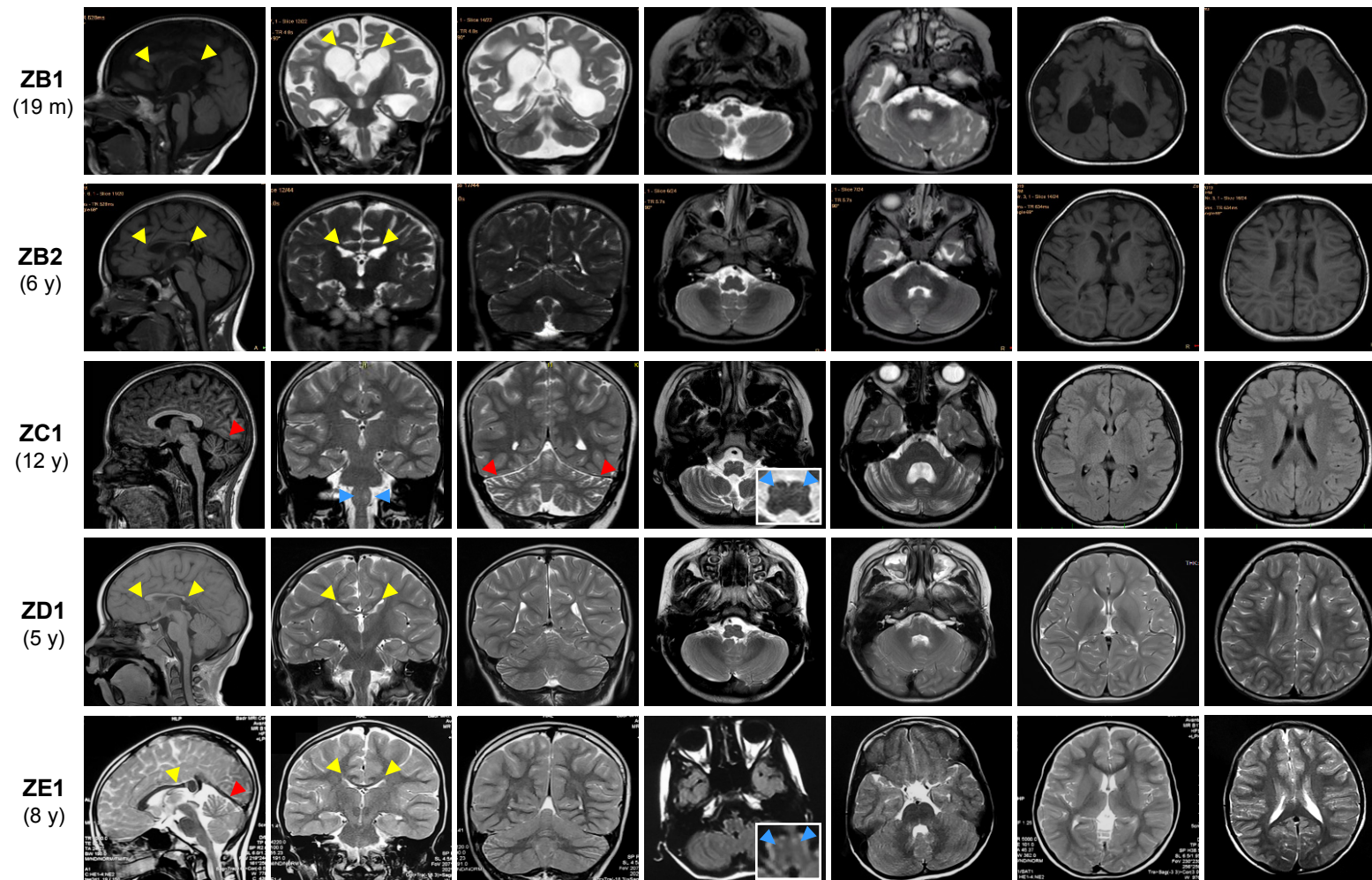
Supplementary Fig. 3 Neuroimaging in subjects with biallelic *HPDL* variants (*continued from previous page*).

Brain MRI studies were normal in subjects with mild disease (individuals F1, T1, and T3) and showed structural changes in subjects with intermediate (individuals C1, D1, ZA1, ZC1, and ZE1) and severe (individuals ZB1, ZB2, and ZD1) disease. Red arrowheads: cerebellar atrophy; blue arrowheads: hyperintensities on T2-weighted images; yellow arrowheads: hypoplasia or dysplasia of the corpus callosum. Note ventriculomegaly (individual ZB1), global cerebral atrophy (individuals ZB1 and ZB2), simplified gyral pattern (individuals ZB1 and ZB2) and generalized reduction of white matter volume (individuals ZB1, ZB2, and ZD1) in severely affected subjects. Age at examination is given in months (m) or years (y).
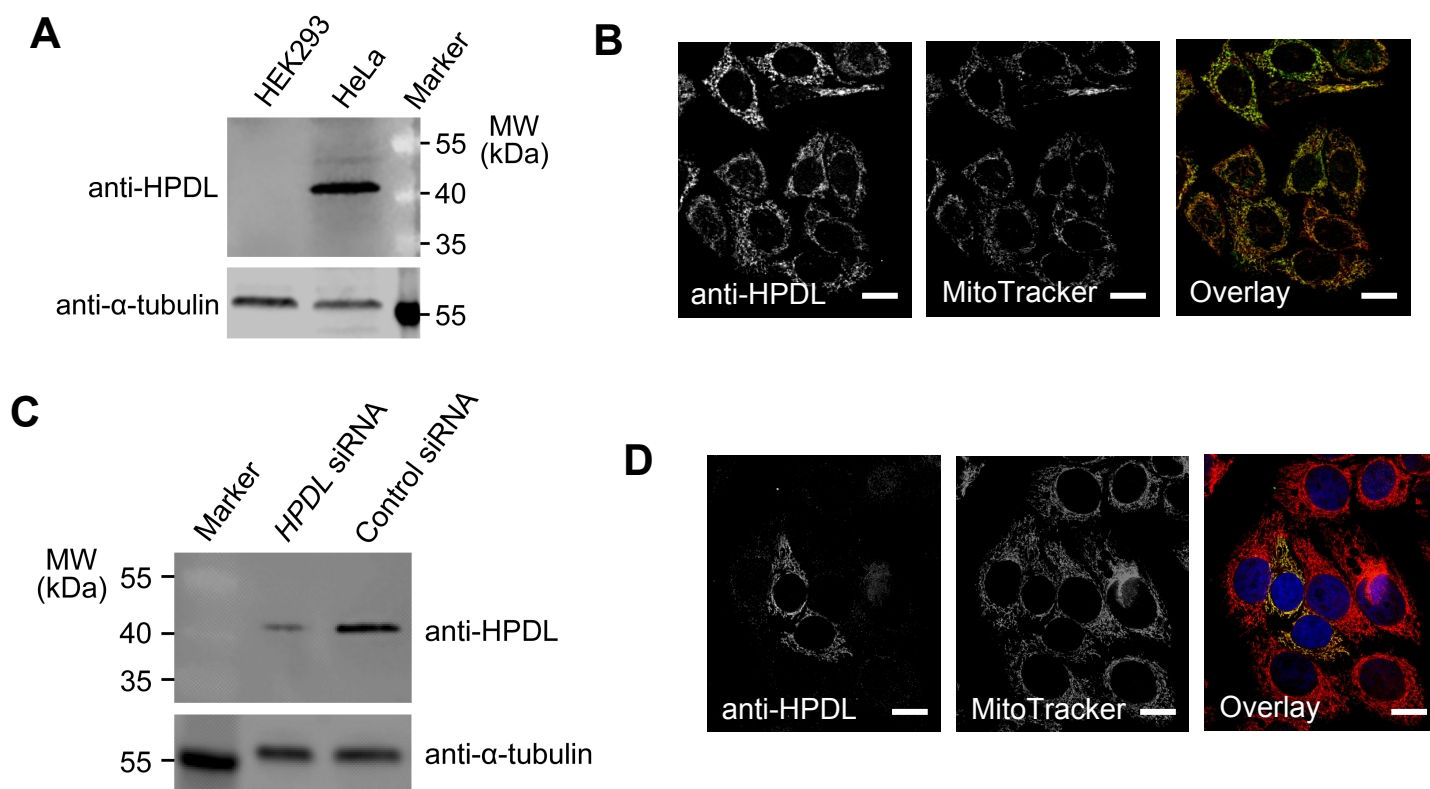
Supplementary Fig. 4 Validation of a rabbit anti-HPDL antibody (Proteintech #20777-1-AP).

Untreated HeLa and HEK293 cells as well as HeLa cells transfected with *HPDL* siRNA or non-targeting control siRNA (50 nM, Riboxx) were lysed in RIPA buffer. Protein extracts were run on SDS gels and blotted onto PVDF membranes. Protein bands were visualized by detection with primary (rabbit anti-HPDL, rabbit anti-α-tubulin) and secondary (IRDye-conjugated anti-IgG) antibodies and infrared fluorescence imaging.

Untreated HeLa cells and HeLa cells transfected with *HPDL* siRNA (50 nM, Riboxx) were labeled with MitoTracker Red (Invitrogen), fixed in 4% PFA in PBS for 10 min, permeabilized with 0.1% Triton X-100 in PBS for 15 min and blocked with 5% horse serum in PBS for 1 h. Cells were stained with primary (rabbit anti-HPDL) and secondary (Alexa Fluor-conjugated anti-IgG) antibodies.

(A) Immunoblot detection of endogenous HPDL in HEK293 and HeLa cells. A specific signal was observed in in HeLa cells while no signal was seen in HEK293 cells.

(B) Immunofluorescence detection of endogenous HPDL in HeLa cells. Co-staining with MitoTracker Red indicated mitochondrial localization of HPDL. Scale bar = 15 μm.

(C) Immunoblot detection of HPDL in HeLa cells treated with an siRNA directed against the *HPDL* mRNA. HPDL levels are clearly decreased compared to cells treated with a control siRNA.

(D) Immunofluorescence detection of HPDL in siRNA-treated HeLa cells. Most cells show no detectable level of HPDL. The transfection rate was about 70%. Scale bar = 15 μm.

A

B
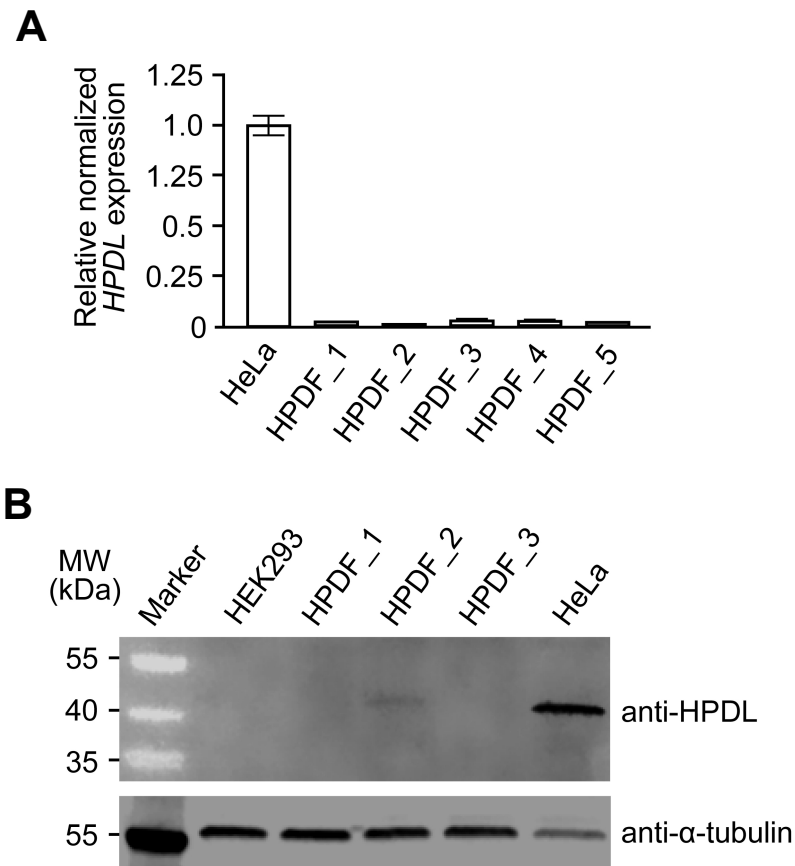
Supplementary Fig. 5 Detection of HPDL in cell lines and human primary dermal fibroblasts.

RNA was isolated from HeLa cells and human primary dermal fibroblasts (HPDF) with the RNeasy Mini Kit (Qiagen) and and reverse transcribed with the PrimeScript RT Kit (Takara). Quantitative PCR was performed with the SYBR Green system (Applied Biosystems). *HPDL* levels were normalized to *GAPDH* and results were expressed as means and SD of three experiments.

Total protein was extracted from HeLa, HEK293 and fibroblast cells with RIPA buffer, run on SDS gels and transferred to PVDF membranes. Protein bands were visualized by detection with primary (rabbit anti-HPDL, rabbit anti-α-tubulin) and secondary (IRDye-conjugated anti-IgG) antibodies and infrared fluorescence imaging.

(A) *HPDL* expression in HeLa cells and HPDF obtained from five healthy donors. In fibroblasts, *HPDL* expression was below the detection threshold of the RT-PCR assay. Bars correspond to means and error bars represent SD of three experiments.

(B) Immunoblot detection of endogenous HPDL in HeLa and HEK293 cells and HPDF obtained from three healthy donors. A specific band was observed in HeLa cells while fibroblasts and HEK293 cells yielded no clearly detectable signal.
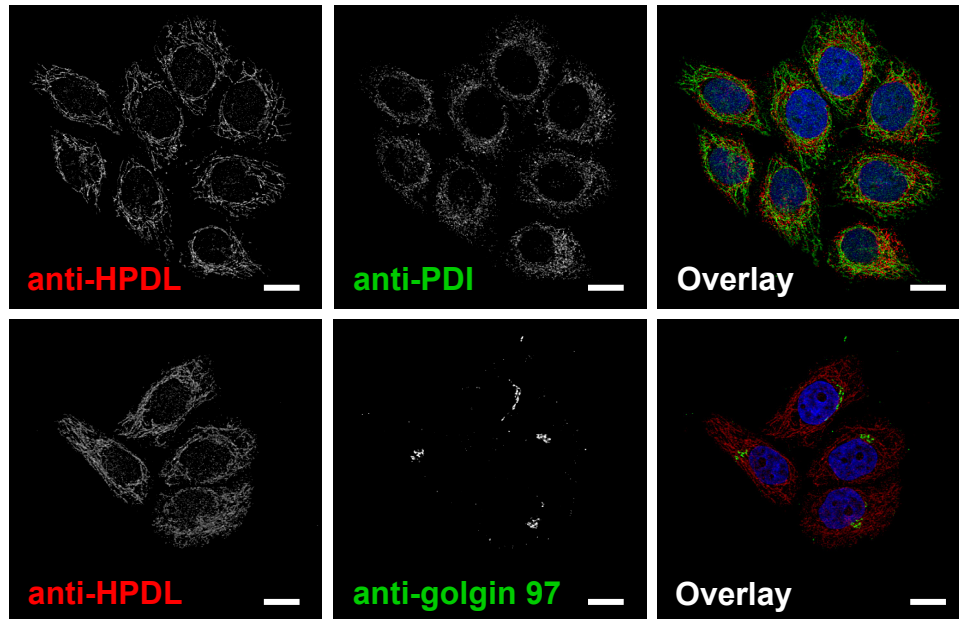
Supplementary Fig. 6 Localization studies with endogenous HPDL and organelle markers.

HeLa cells were fixed in 4% PFA in PBS for 10 min, permeabilized with 0.1% Triton X-100 in PBS for 15 min and blocked with 5% horse serum in PBS for 1 h. Cells were then stained with primary (rabbit anti-HPDL, mouse anti-PDI (Stressgen #SPA-891 (1D3); 1:200), mouse anti-golgin 97 (Thermo Fisher #A-21270 (CDF4); 1:500)) and secondary (Alexa Fluor-conjugated anti-IgG) antibodies. Images were captured with a Zeiss Axiovert 200 M microscope.

Endogenous HPDL showed only minor overlap with signals for the endoplasmic reticulum marker PDI and the Golgi apparatus marker golgin 97. Scale bar = 10 μm.
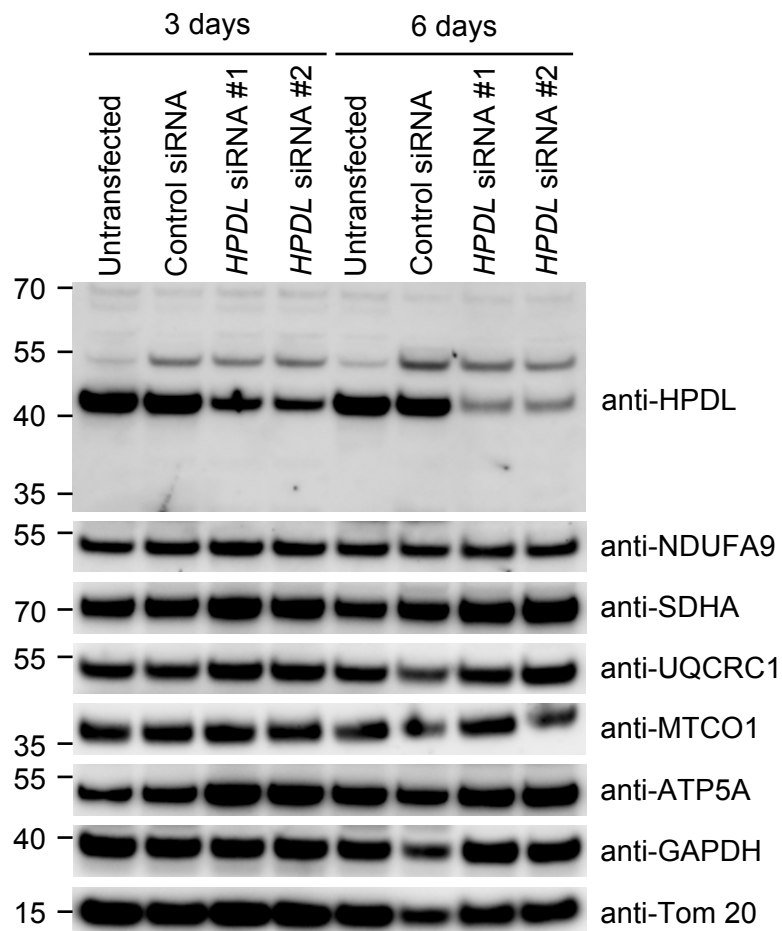
Supplementary Fig. 7 Levels of subunits of mitochondrial respiratory chain complexes in HPDL-siRNA treated HeLa cells.

HeLa cells were seeded at a density of $2x10^5$ cells/well in 6-well plates. After 24 h, cells were transfected with 50 nM HPDL or non-targeting control siRNA (Riboxx) with Lipofectamine (Invitrogen). On day 3 after transfection, total protein was extracted with RIPA buffer or cells were transfected for a second time with the same siRNA and protein was extracted on day 6. Protein extracts run on SDS gels and transferred to PVDF membranes. Specific bands were visualized by immuno-detection with primary (mouse anti-NDUFA9, mouse anti-SDHA, mouse anti-UQCRC1, mouse anti-MTCO1, mouse anti-ATP5A, rabbit anti-Tom 20, mouse anti-GAPDH, rabbit anti-HPDL) and secondary (HRP-conjugated anti-IgG) antibodies and recording of ECL (Thermo Fisher) chemiluminescence.

Immunoblot detection of NDUFA9 (complex I), SDHA (complex II), UQCRC1 (complex III), MTCO1 (complex IV), and ATP5A (complex V) in protein extracts from Hela cells did not reveal major effects of HPDL depletion on the levels of subunits of the mitochondrial respiratory chain. Efficient knockdown was monitored using the specific anti-HPDL antibody. Tom 20 (protein of the outer mitochondrial membrane) served as a marker for mitochondrial mass.
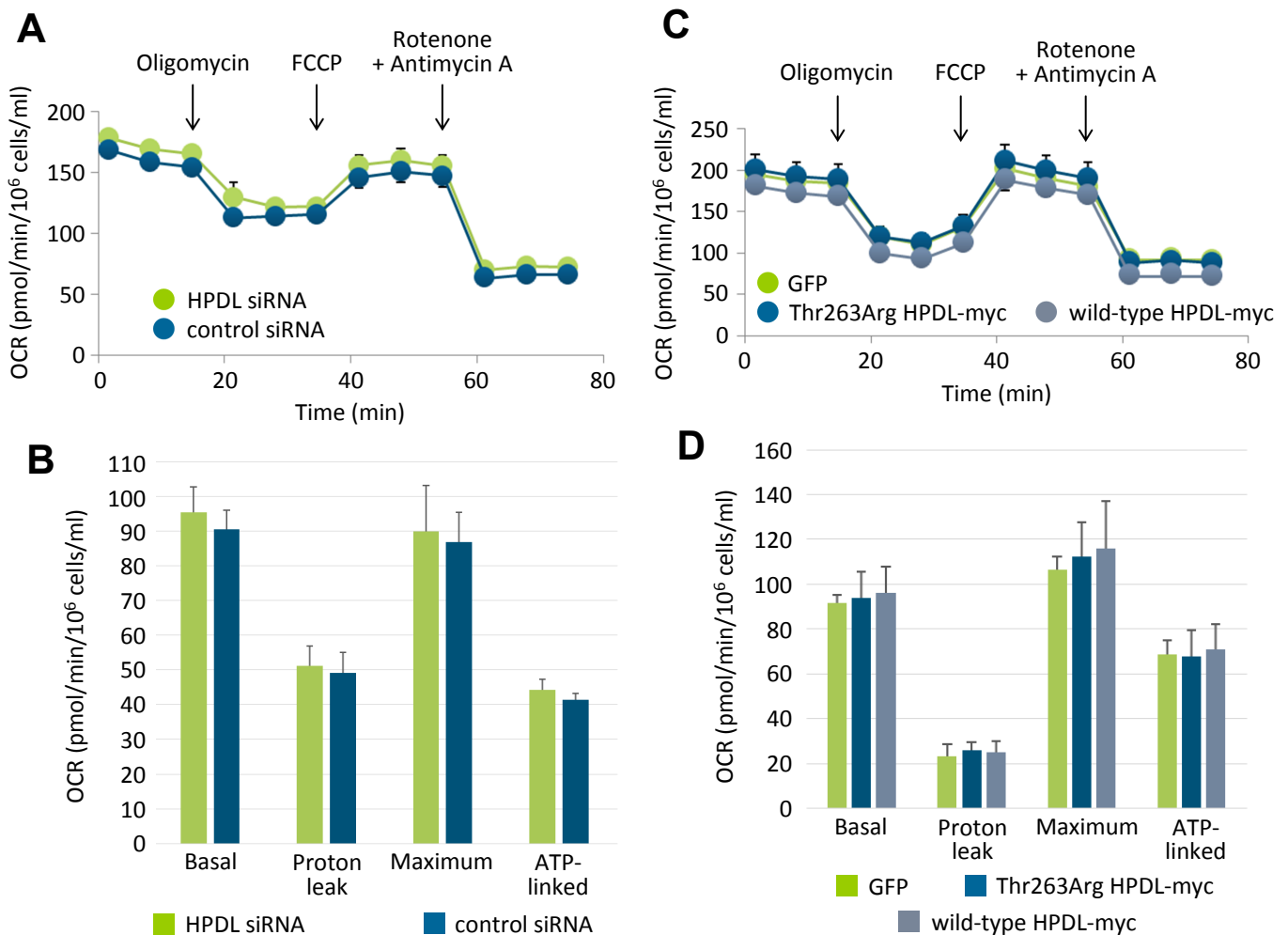
**Supplementary Fig. 8** Respiratory profile of HeLa cells expressing different levels of HPDL.

HeLa cells were seeded at a density of 2x105 cells/well in 6-well plates. After 24 h cells were transfected with 50 nM HPDL or non-targeting control siRNA (Riboxx) or with HPDL-myc or GFP control plasmids. One day after transfection, $1.2x10^4$ cells/well were seeded in XFp Cell Culture Miniplates (Seahorse). The next day, the culture medium was replaced by Basal Assay Medium (1 mM pyruvate, 2 mM glutamine, 10 mM glucose). One h before starting the assay, cells were incubated at 37 ºC without CO_2. Oxygen consumption rate (OCR) was determined on a Seahorse Bioscience XFp Extracellular Flux Analyzer at baseline and after injection of pharmacological manipulators of the mitochondrial respiratory chain (ATP synthase inhibition by Oligomycin (1.0 μM), oxidative phosphorylation uncoupling by FCCP (0.5 μM), complete inhibition of mitochondrial respiration by Rotenone + Antimycin A (0.5 μM)). Data were analyzed with Seahorse Wave software and expressed as means and SEM from triplicate wells.

(A) OCR in HeLa cells transfected with HPDL siRNA and control siRNA. OCR over time was measured to test effects of pharmacological manipulators of the mitochondrial respiratory chain Oligomycin, FCCP, Rotenone + Antimycin A.

(B) Bar diagrams showing mitochondrial bioenergetics parameters (basal mitochondrial OCR, OCR attributed to proton leak, maximum OCR, and ATP-linked OCR) in HeLa cells transfected with HPDL siRNA or control siRNA.

(C) OCR in HeLa cells transfected with HPDL expression constructs or an control plasmid containing GFP. OCR over time was measured to test effects of pharmacological manipulators of the mitochondrial respiratory chain Oligomycin, FCCP, Rotenone + Antimycin A.

(D) Bar diagrams showing mitochondrial bioenergetics parameters in HeLa cells transfected with HPDL expression constructs or an control plasmid containing GFP.
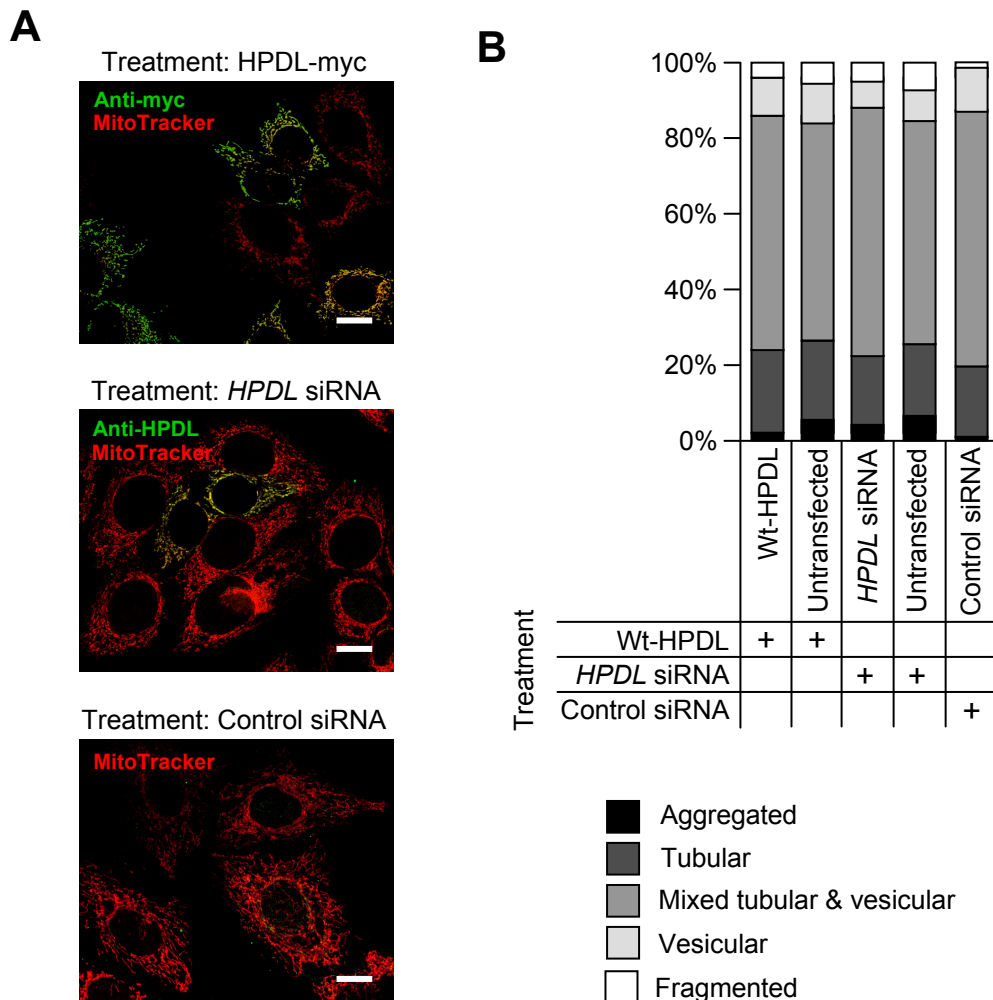
Supplementary Fig. 9 Mitochondrial morphology in HPDL-depleted Hela cells and HeLa cells overexpressing HPDL.

HeLa cells transfected with an HPDL-myc expression construct or 50 nM *HPDL* siRNA or non-targting control siRNA (Riboxx) were labeled with MitoTracker Red (Invitrogen), fixed in 4% PFA in PBS for 10 min, permeabilized with 0.1% Triton X-100 in PBS for 15 min and blocked with 5% horse serum in PBS for 1 h. Transfected cells expressing HPDL-myc were detected with mouse anti-myc primary and Alexa Fluor-conjugated anti-IgG secondary antibodies. HPDL knockdown in siRNA treated cells was monitored with rabbit anti-HPDL primary and Alexa Fluor-conjugated anti-IgG secondary antibodies. Mitochondrial morphology was categorized according to a published protocol (Niemann *et al.*, 2005).

(A) Most mitochondria (labelled with MitoTracker Red) showed a mixed tubular and vesicular aspect, largely indistinguishable between transfected and untransfected cells. Scale bar = 10 μm.

(B) Results were quantified by categorizing the appearance of mitochondria (aggregated, tubular, mixed tubular and vesicular, vesicular, fragmented). At least 100 cells were counted for the following five conditions: (1) HPDL-myc overexpressing cells and (2) interspersed cells without myc signals on the same coverslip; (3) HPDL-siRNA treated cells with efficient knockdown and (4) interspersed cells with retained HPDL signals on the same coverslip; (5) control-siRNA treated cells.
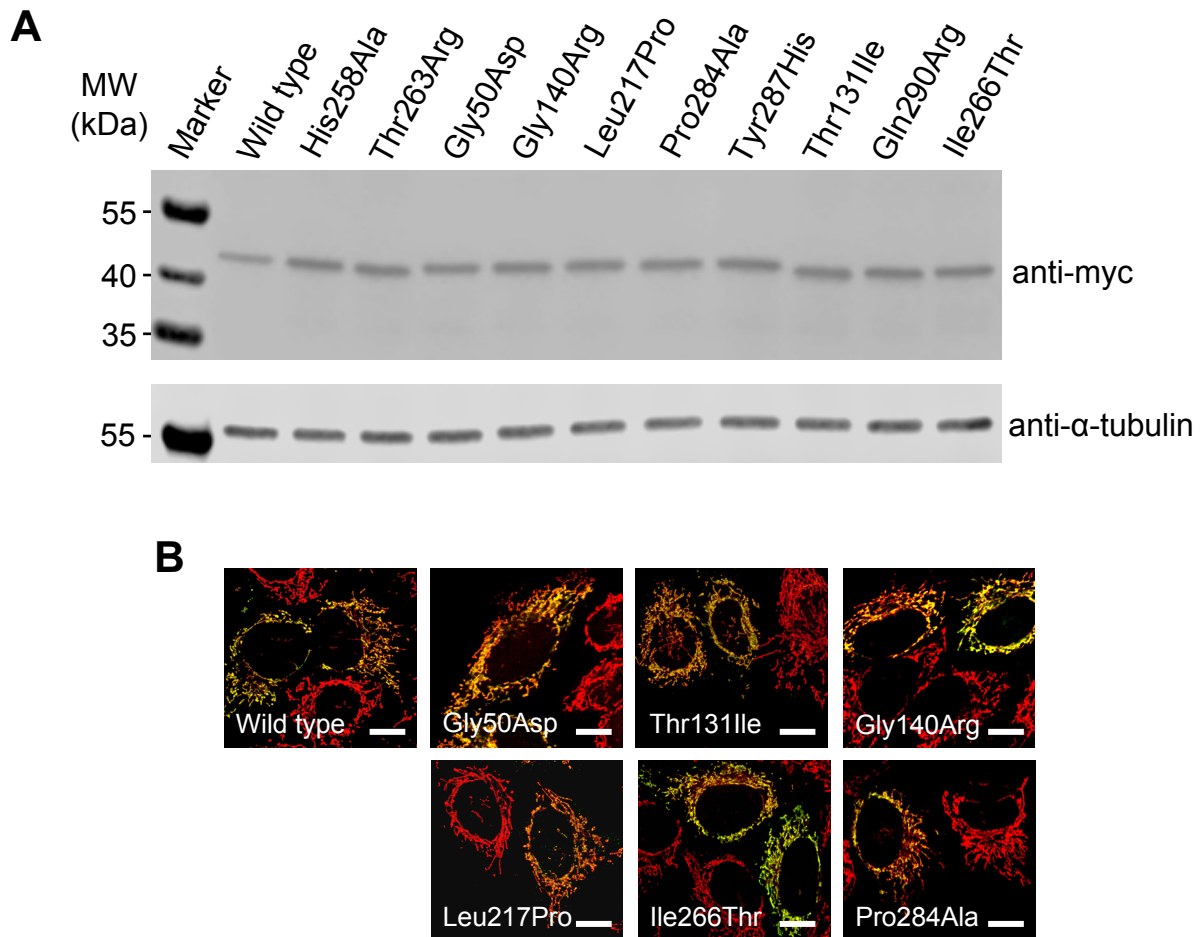
Supplementary Fig. 10 Protein levels and subcellular localization of HPDL missense variants.

Total protein was extracted from HPDL-myc-transfected HeLa cells with RIPA buffer, run on SDS gels and transferred to PVDF membranes. Protein bands were visualized by detection with primary (mouse anti-myc, rabbit anti-α-tubulin) and secondary (IRDye-conjugated anti-IgG) antibodies and infrared fluorescence imaging.

HPDL-myc-transfected HeLa cells were labeled with MitoTracker Red, fixed in 4% PFA in PBS for 10 min, permeabilized with 0.1% Triton X-100 in PBS for 15 min and blocked with 5% horse serum in PBS for 1 h. Cells were stained with primary (mouse anti-myc) and secondary (Alexa Fluor-conjugated anti-IgG) antibodies.

(A) Immunoblot analysis of protein extracts from HeLa cells transfected with expression constructs encoding myc-tagged HPDL yielded comparable levels of wild-type and mutant HPDL species. Thr131Ile, His258Ala, Pro284Ala and Gln290Arg are artificial mutants representing alterations of invariant (Thr131, His258 and P284) or less stringently conserved (Gln290) amino acids.

(B) Immunofluorescence microscoppy and detection of overexpressed protein with an anti-myc antibody (green signal) showed regular mitochondrial localization of all mutants tested (red signal: mitochondrial marker MitoTracker Red). Interspersed untransfected cells are shown for comparison. Scale bar = 10 µm.
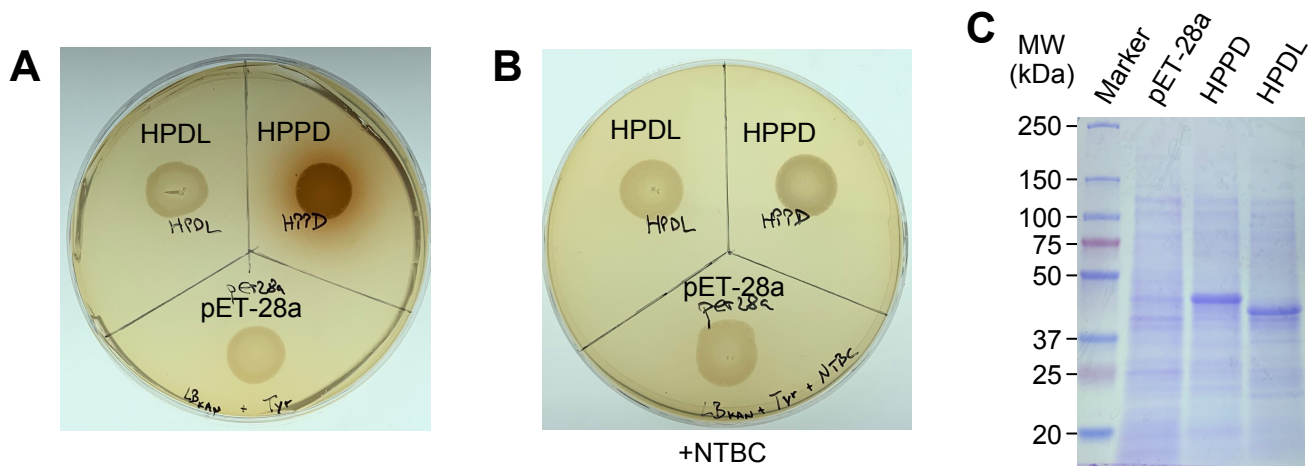
Supplementary Fig. 11 Enzymatic activity of bacterially expressed HPPD and HPDL.

Recombinant E. coli expressing HPDL or HPPD (in pET-28a) were grown in LB medium with 50 mg/ml kanamycin. Total protein was extracted by sonication of cells in lysis buffer (10 mM Tris-HCl, 1% SDS, pH 7.5) and run on SDS gels. Protein bands were visualized by Coomassie staining.

Recombinant E. coli expressing HPDL or HPPD were grown on LB plates with 50 mM tyrosine and 50 mg/ml kanamycin. Enzyme activity was assessed by formation of a brownish pigment. NTBC (nitisinone) was used to inhibit HPPD activity.

(A) Recombinant *E. coli* expressing the HPDL-orthologue HPPD produce a brownish pigment when growing on medium supplemented with tyrosine. Alternatively, neither expression of HPDL instead of HPPD nor the empty vector-control (pET-28a) lead to pigment formation.

(B) No brown color is observed after addition of the HPPD inhibitor NTBC (nitisinone), implying that the pigment indeed resulted from the HPPD reaction.

(C) Appropriate levels of HPPD and HPDL in bacteria were confirmed by gel electrophoresis of protein extracts and subsequent Coomassie blue staining.

13

```
                                                          ▽                              ▼
  6  LRLCHIAFHVPAGQPLARNLQRLFGFQPLASREVD-GWRQLA---LRSGDAVFLVNEGAG
 17  LHFHSVTFWVGNAKQAASFYCSKMGFEPLAYRGLETGSREVVSHVIKQGKIVFVLSSALN

                            ▽
 62  SGEPLYGLDPRHAVPSATNLCFDVADAGAATRELAALGCSVPVPPVRVRDAQGAATYAVV
 77  PWNKEMGDHLVKHGDGVKDIAFEVEDCDYIVQKARERGAKIMREPWVEQDKFGKVKFAVL

                         ▼                                    *  ▽   ▽       ▽
122  SSPAGILSLTLLERAGYRGPFLPGFR------PVSSAPGPGWVSRVDHLTLACTPGSSPT
137  QT-YGDTTHTLVEKMNYIGQFLPGYEAPAFMDPLLPKLPKCSLEMIDHIVGNQPDQEMVS

           ▽                                  ▼                       ▽
176  LLRWFHDCLGFCHLPLSPGEDPELGLEMTAGFGLGGLRLTALQAQPGSIVPTLVLAESLP
196  ASEWYLKNLQFHRF--WSVDDTQVHTEYSS------LRSIVVANYEESI--KMPINEPAP

              *            ▽    ▼                           ▽     ▼
236  GATTRQDQVEQFLARHKGPGLQHVGLYTPNIVEATEGVATAGGQFLAPPGAYYQQPGKER
246  GK--KKSQIQEYVDYNGGAGVQHIALKTEDIITAIRHLRERGLEFLSVPSTYYKQLREKL

                                                ▽*
296  QIRAAGHEPHL--LARQGIILDGDKGKFLLQVFTKSLFTEDTFFLELIQRQGATGFGQGN
304  KTAKIKVKENIDALEELKIIVDYDEKGYLLQIFTKPVQDRPTLFLEVIQRHNHQGFGAGN

            ▽
354  IRALWQSVQEQ     364
364  FNSLFKAFEEE     374
```

Supplementary Fig. 12 Sequence alignment of human HPDL and HPPD.

Human HPDL (UniProt Q96IR7) and human HPPD (UniProt P32754) sequences were aligned using CLUSTALW with default parameters.

Alignment of the HPDL (top line) and HPPD (bottom line) sequences. Asterisks indicate amino acids that coordinate the iron atom in the catalytic center of HPPD. Residues altered by *HPDL* missense variants in our cohort of HSP subjects are indicated by arrowheads. Filled arrowheads: variants tested in the enzymatic assay (**Fig. 3A**, **Fig. 3B**).
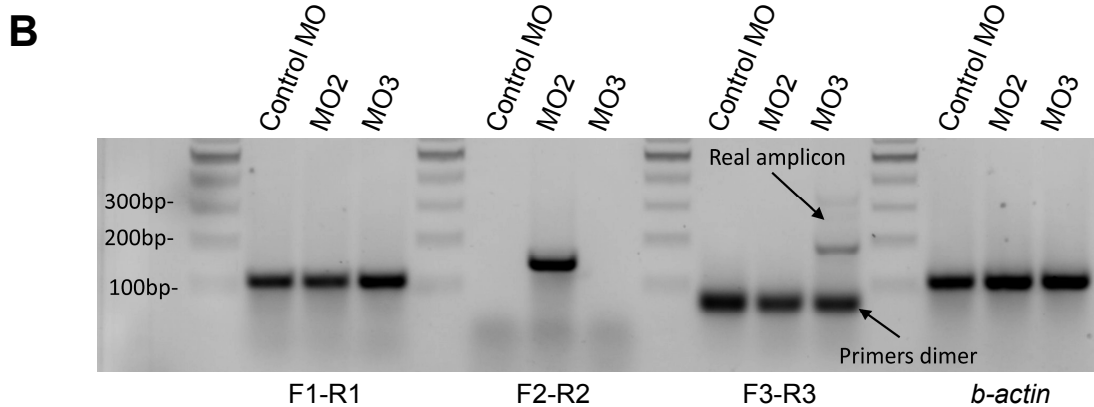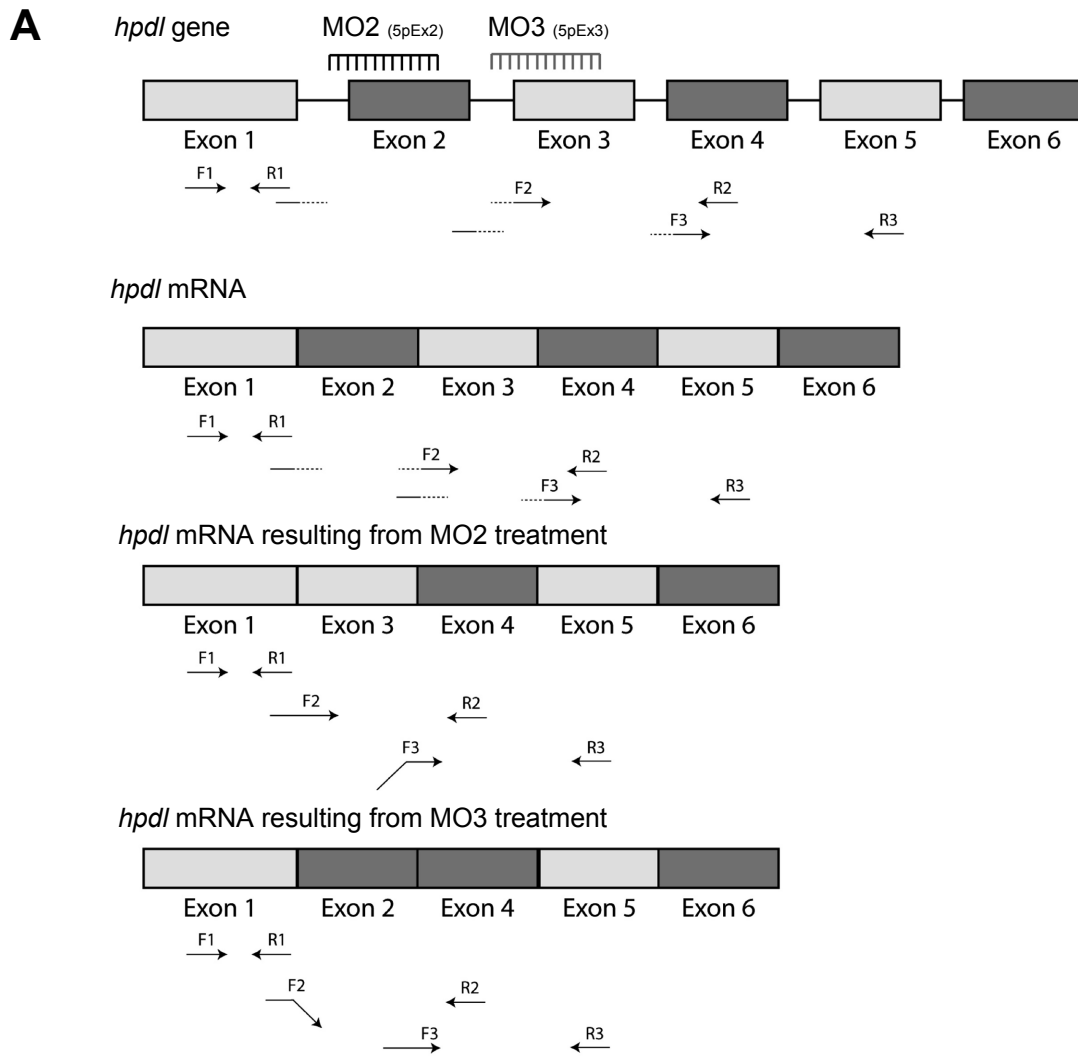
Supplementary Fig. 13 Knockdown of zebrafish *hpdl*.

Sequences of two MOs interfering with splicing of the *hpdl* transcript were defined using sequence information from ZFIN (ZDB-GENE-071004-50). MOs targeting *hpdl* or a control MO (Genetools) were injected in single-cell embryos and RNA was extracted at the larval stage (5 dpf). RNA was reverse transcribed into cDNA which was then used for PCR with primers shown in (A). PCR products were run on agarose gels and visualized by ethidium bromide staining.

(A) Positions of MOs and RT-PCR primers. MO2 and MO3 block acceptor splice sites of introns 2 and 3, respectively. Primers F1-R1 amplify all transcripts irrespective of MO activity while F2-R2 and F3-R3 only amplify transcripts with exon 1-3 (MO2) or exon 2-4 junctions (MO3).

(B) MO-induced mis-splicing of the *hpdl* transcript. RT-PCR with primer sets specified in (A) demonstrated that the MOs affected *hpdl* splicing as expected. *b-actin*: amplification control.

15
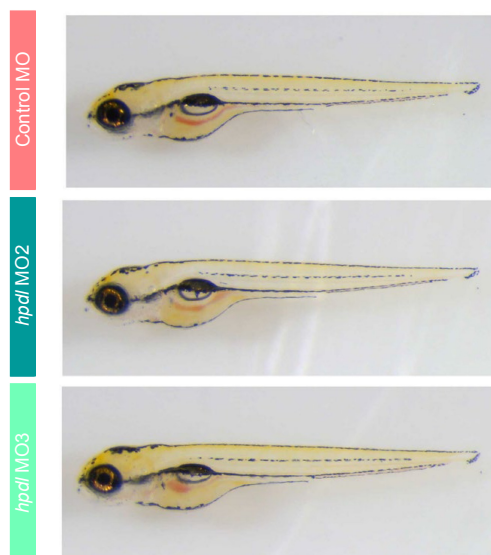
Supplementary Fig. 14 Gross anatomy of morpholino-treated zebrafish.

MO targeting *hpdl* or a control MO were injected in single-cell embryos and fish were used for imaging at the larval stage (5 dpf). Images were taken with a stereomicroscope equipped with a digital camera (Leica).

Analysis of control fish (control MO-injected), *hpdl* MO2-injected embryos and *hpdl* MO3-injected embryos showed no macroscopic differences between the three conditions.
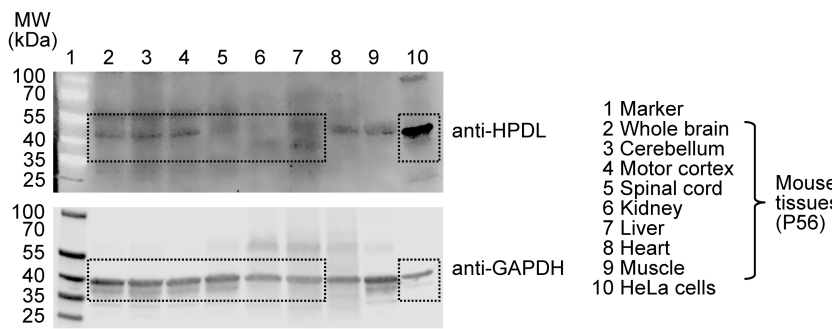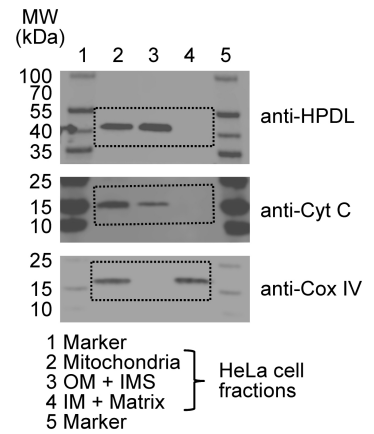
Figure 2B

MW (kDa)

1 2 3 4 5 6 7 8 9 10
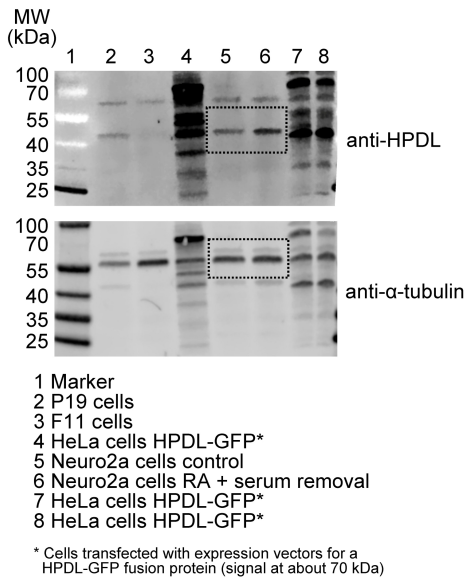
100
70
55
40
35
25

anti-HPDL

100
70
55
40
35
25

anti-GAPDH

1 Marker
2 Whole brain
3 Cerebellum
4 Motor cortex
5 Spinal cord
6 Kidney
7 Liver
8 Heart
9 Muscle
10 HeLa cells

Mouse tissues (P56)

Figure 2F (upper panel)

MW (kDa)

1 2 3 4 5

100
70
55
40
35

anti-HPDL

25
15
10

anti-Cyt C

25
15
10

anti-Cox IV

1 Marker
2 Mitochondria
3 OM + IMS
4 IM + Matrix
5 Marker

HeLa cell fractions

Figure 2D

MW (kDa)

1 2 3 4 5 6 7 8

100
70
55
40
35
25

anti-HPDL

100
70
55
40
35
25

anti-α-tubulin

1 Marker
2 P19 cells
3 F11 cells
4 HeLa cells HPDL-GFP*
5 Neuro2a cells control
6 Neuro2a cells RA + serum removal
7 HeLa cells HPDL-GFP*
8 HeLa cells HPDL-GFP*

* Cells transfected with expression vectors for a HPDL-GFP fusion protein (signal at about 70 kDa)

Figure 2F (left lower panel)

MW (kDa)

1 2 3 4 5

100
70
55
40
35

anti-HPDL

25
15
10

anti-Tom 20

25
15
10

anti-Cox IV

1 Marker
2 Untreated
3 Proteinase K
4 Proteinase K + SDS
5 Marker

HeLa cell mitochondria
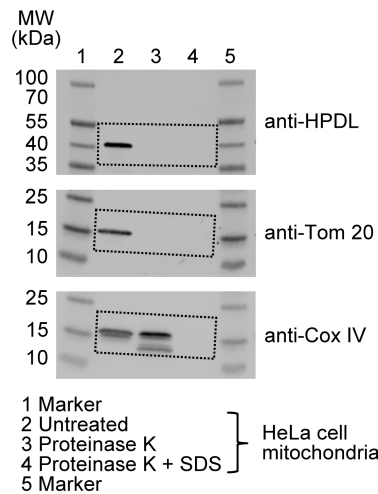
Figure 2F (right lower panel)

MW (kDa)

1 2 3 4

55
40
35
25
15
10

anti-HPDL

1 Marker
2 Untreated
3 Proteinase K
4 Proteinase K + SDS

HeLa cell mitochondria

Figure 2E

MW (kDa)

1 2 3 4 5 6 7

100
70
55
40
35
25
15

anti-HPDL

100
70
55

anti-α-tubulin

100
70
55

anti-PDI

25
15

anti-Cox IV

1 Marker
2 No sample loaded
3 Nuclei and cell debris
4 Mitochondria
5 Cytosol
6 PM and ER
7 Marker

Figure 3A

MW (kDa)

1 2 3 4 5 6 7 8 9 10 11 12 13 14 15

130
95
55
43
34
26

anti-HPPD

1 Marker*
2 HPPD protein purified from *E. coli*
3 WT
4 WT + inhibitor
5 Gln375Asn
6 Arg378Lys
7 Gly65Asp
8 Thr145Ile
9 Gly154Arg
10 Val229Pro
11 Thr271Arg
12 Ile274Thr
13 Pro292Ala
14 Tyr295His
15 Marker

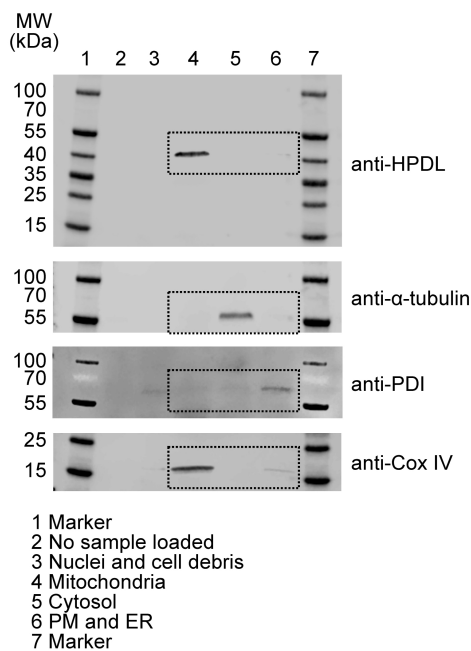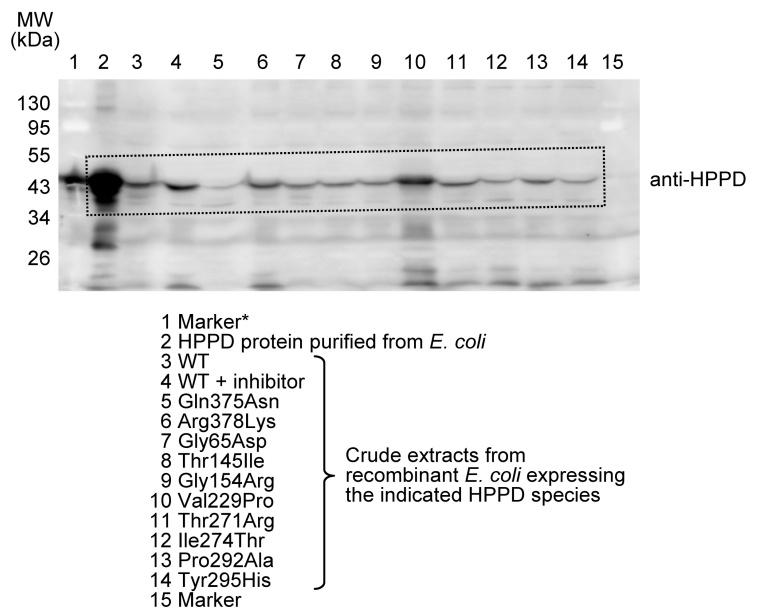Crude extracts from recombinant *E. coli* expressing the indicated HPPD species

* The signal at the size of the HPPD band results from spillover from lane 2 (purified HPDL protein).

Supplementary Fig. 15 Uncropped versions of western blots.

Supplementary Table 1 Antibodies used in this study

Antigen	Source	Manufacturer	Catalogue number	Clone	Dilution	2nd antibody conjugates
Western blotting						
α-tubulin	rabbit	Cell Signaling	#2144		1:500	IRDye[1]
ATP5A	mouse	Abcam	#ab14748	15H4C4	1:1,000	HRP[2]
Cox IV	rabbit	Cell Signaling	#4850	3E11	1:1,000	IRDye[1]
Cyt C	mouse	Abcam	#ab13575	7H8.2C12	1:2,000	IRDye[1]
GAPDH	mouse	Merck Millipore	#CB1001	6C5	1:500	IRDye[1], HRP[2]
HPDL	rabbit	Proteintech	#20777-1-AP		1:1,000	IRDye[1], HRP[2]
HPPD	rabbit	Proteintech	#17004-1-AP		1,000	HRP[2]
MTCO1	mouse	Abcam	#ab14705	1D6E1A8	1:1,000	HRP[2]
NDUFA9	mouse	Abcam	#ab14713	20C11B11B11	1:1,000	HRP[2]
PDI	mouse	Stressgen	#SPA 891D	1D3	1:1,000	IRDye[1]
SDHA	mouse	Abcam	#ab14715	2E3GC12FB2AE2	1:2,000	HRP[2]
Tom 20	mouse	Santa Cruz	#sc-17764	F-10	1:500	IRDye[1]
Tom 20	rabbit	Abcam	#186735	EPR15581-54	1:2,000	HRP[2]
UQCRC1	mouse	Abcam	#ab110252	16D10AD9AH5	1:1,000	HRP[2]
Immunofluorescence microscopy						
calbindin	mouse	Sigma Aldrich	#C9848	CB-955	1:400	Alexa Fluor[3]
golgin 97	mouse	Thermo Fisher	#A-21270	CDF4	1:500	Alexa Fluor[3]
HPDL	rabbit	Proteintech	#20777-1-AP		1:100	Alexa Fluor[3]
myc	mouse	Clontech	#631206	9E10	1:200	Alexa Fluor[3]
PDI	mouse	Stressgen	#SPA-891	1D3	1:200	Alexa Fluor[3]

[1]IRDye-conjugated anti-IgG antibodies (Rockland)
[2]HRP-conjugated anti-IgG antibodies (Sigma Aldrich)
[3]Alexa Fluor-conjugated anti-IgG antibodies (Invitrogen)

Supplementary Table 2 Genes highlighted by linkage analysis and ES in families A and B

Family	Gene	Variant	MAF gnomAD all exomes	Conservation	CADD	Gene function	Disease link	Neural expression[1]
A	*PTPRF*	p.Met1564Val	2.790e-05	strong	damaging	protein tyrosine phosphatase	AR athelia	yes
A	*HPDL*	p.Gly50Asp	1.018e-05	strong	damaging	tyrosine metabolism (?)	none	yes
A	*RIT2*	p.Lys184del	1.990e-05	strong	n.a.	Ras family member	none	yes
A	*ZCCHC2*	p.Gln536Arg	2.810e-05	strong	damaging	transcription factor (?)	none	yes
B	*TCTEX1D4*	p.Ala130Ser	1.309e-03	moderate	tolerated	inhibition of TGFB signaling (?)	none	no
B	*ZSWIM5*	p.Cys423Arg	0	strong	damaging	transcription factor (?)	none	yes
B	*HPDL*	p.Gly140Arg	0	strong	damaging	tyrosine metabolism (?)	none	yes
B	*ALG14*	p.Ser38Ile	2.00e-03	moderate	tolerated	N-linked glycosylation	AR congenital myasthenic syndrome	yes

[1]According to GTEx (https://www.gtexportal.org/home) (GTEx Consortium, 2013)
AR = autosomal recessive; n.a. = not available

Supplementary Table 3 Clinical, neuroimaging and laboratory findings in individuals with biallelic *HPDL* variants

Family	A		B			C	CS1	CS2	CS3
Country of origin / Consanguinity	Syria / Yes		Turkey / Yes			Morocco / No	USA / No	USA / No	USA / No
***HPDL* cDNA variant(s)**	c.149G>A (hom.)		c.418G>A (hom.)			c.518C>A / c.788C>G	c.859T>C / c.847C>T	c.1013T>C / c.769_771delinsTC	c.797T>C / c.503G>A
HPDL protein variant(s)	p.Gly50Asp (hom.)		p.Gly140Arg (hom.)			p.Ser173Tyr / p.Thr263Arg	p.Tyr287His / p.Pro283Ser	p.Leu338Pro / p.Gln257fs	p.Ile266Thr / p.Cys168Tyr
Individual	A1	A2	B1	B2	B3	C1	CS1	CS2	CS3
Sex / age at diagnosis / age at examination	F / 3y / 16 y	M / 12 y / 14 y	F / toddler age / 36 y	M / toddler age / 30 y	M / 5 y / 6 y	M / 6 y / 36 y	F / 17 y / 18 y	F / 4 m / 4y	M / 17 y / 18 y
First symptom(s)	Spastic gait	Spastic gait	LL spasticity	LL spasticity	Spastic gait	Spastic gait	Gait problems, LL stiffness, frequent falls	GDD, infantile spasms, hyps-arrhythmia	Gait problems, LL stiffness, frequent falls
Disease severity / course	Intermediate / progressive	Mild / slowly progressive	Intermediate / progressive	Intermediate / progressive	Intermediate / n.e.	Intermediate / progressive	Mild / n.e.	Severe / non-progressive	Mild / n.e.
Motor delay / best motor ability reached	No / walking	No / walking	No / walking	Yes / walking	No / walking	No / walking	No / walking	Yes / sitting	No / walking
Cognitive delay	No	No	No	Yes	No	No	No	Yes	No
Spastic gait	Yes	Yes	Yes	Yes	Yes	n.e. (wheelchair)	Yes	n.e. (no walking)	Yes
UL pyramidal signs / spasticity / weakness	Yes / No / No	Yes / No / No	Yes / Yes / No	Yes / Yes / No	Yes / No / No	No / No / No	No / No / No	Yes / Yes / Yes	No / No / No
LL pyramidal signs / spasticity / weakness	Yes / Yes / Yes	Yes / Yes / Yes	Yes / Yes / n.a.	Yes / Yes / n.a.	Yes / Yes / n.a.	Yes / Yes / Yes	Yes / Yes / Yes	Yes / Yes / Yes	Yes / Yes / Yes
Pseudobulbar signs	No	No	No	No	No	Yes	No	No	No
Bladder dysfunction	No	No	Yes	Yes	No	n.a.	No	n.a.	No
Ataxia	Yes	Yes	Yes	Yes	No	Yes	No	No	No
Encephalopathic episodes	No	No	No	No	No	Yes (single attack at age 23 y; diagnosed as ADEM)	No	No	No
Contractures	No	No	Yes	Yes	No	n.a.	No	Yes	No
Seizures	No	No	Yes	Yes	No	No	No	Yes	No
Oculomotor abnormalities	No	No	Yes	Yes	No	Yes	No	Yes	No
Brain MRI (age at examination)	Cerebellar atrophy (n.a.)	n.a.	Thinning of the CC (n.a.)	Thinning of the CC (n.a.)	n.a.	Dysplastic CC, cerebellar atrophy, T2 hyperintensities in the medulla oblongata (34 y)	Normal (n.a.)	Mild supratentorial atrophy and hypo-myelination (n.a.)	Normal (n.a.)
Spinal MRI (age at examination)	n.a.	n.a.	n.a.	n.a.	n.a.	Normal (25 y)	Normal (n.a.)	n.d.	Normal (n.a.)
Muscle RC complex / blood / CSF lactate	n.a. / n.a. / n.a.	n.a. / n.a. / n.a.	n.a. / n.a. / n.a.	n.a. / n.a. / n.a.	n.a. / n.a. / n.a.	n.d. / n.d. / n.d.	n.d. / Normal / n.d.	n.a. / Normal / n.d.	n.d. / Normal / n.d.
Blood tyrosine / urine organic acids	n.a. / n.a.	n.a. / n.a.	n.a. / n.a.	n.a. / n.a.	n.a. / n.a.	n.d. / n.d.	Normal / Mildly increased4-HPA but normal 4-HPP and 4-HPL	n.a. / n.a.	n.d. / n.d.

Supplementary Table 3 Clinical, neuroimaging and laboratory findings in individuals with biallelic *HPDL* variants (continued from previous page)

Family	CS4	D	E	F	FRL	FRN	T		
Country of origin / Consanguinity	USA / No	Italy / No	Saudi Arabia / Yes	Turkey / Yes	Algeria / No	Algeria / Yes	Egypt / Yes		
***HPDL* cDNA variant(s)**	c.27C>A / c.569C>T	c.797T>C / c.256del	c.256del (hom.)	c.149G>A (hom.)	c.788C>T (hom.)	c.342_345dup (hom.)	c.149G>A (hom.)		
HPDL protein variant(s)	p.Cys9* / p.Pro190Leu	p.Ile266Thr / p.Ala86fs	p.Ala86fs (hom.)	p.Gly50Asp (hom.)	p.Thr263Met (hom.)	p.Ala116fs (hom.)	p.Gly50Asp (hom.)		
Individual	CS4	D1	E1	F1	FRL1	FRN1	T1	T2	T3
Sex / age at diagnosis / age at examination	F / 10 m / 11 m	M / 3 y / 21 y	F / 12 m / n.a.	M / 13 y / 17 y	F / 1 m / 1 y	M / 7 d / 6 y	M / 15 y / 17 y	M / 14 y / 16 y	F / 11 y / 13 y
First symptom(s)	GDD, partial seizures, hypothermia	Stiffness in LL	n.a.	Gait problems	Seizures	Neonatal seizures	Progressive LL weakness	Gait problems, LL stiffness, frequent falls	LL stiffness, frequent falls
Disease severity / course	Severe / episodic deteriorations	Intermediate / progressive	Severe / episodic deteriorations	Mild /slowly progressive	Severe / episodic deteriorations	Severe / non-progressive	Mild / n.e.	Mild / slowly progressive	Mild / slowly progressive
Motor delay / best motor ability reached	Yes / head control	No / walking	Yes / n.a.	No / walking	Yes / head control	Yes / no motor development	No / walking	No / walking	No / walking
Cognitive delay	Yes	No	Yes	No	Yes	Yes	Yes	Yes	No
Spastic gait	n.e. (too young)	n.e. (wheelchair)	n.a.	Yes	n.e. (too young)	n.e. (no walking)	Yes	Yes	Yes
UL pyramidal signs / spasticity / weakness	Yes / Yes / Yes	Yes / No / No	No / No / No	No / No / No	Yes / Yes / Yes	Yes / Yes / Yes	Yes / No / No	Yes / No / No	No / No / No
LL pyramidal signs / spasticity / weakness	Yes / Yes / Yes	Yes / Yes / Yes	Yes / Yes / No	Yes / Yes / Yes	Yes / Yes / Yes	Yes / Yes / Yes	Yes / Yes / Yes	Yes / Yes / Yes	Yes / Yes / No
Pseudobulbar signs	No	Yes	No	No	Yes	n.a.	No	n.a.	n.a.
Bladder dysfunction	n.e. (too young)	No	No	n.a.	n.e. (too young)	n.e. (severe GDD)	No	n.a.	n.a.
Ataxia	No	Yes	No	No	n.e. (severe GDD)	n.e. (severe GDD)	No	n.a.	n.a.
Encephalopathic episodes	Yes	No	Yes	No	Yes	No	No	No	No
Contractures	Yes	Yes	Yes	Yes	Yes	Yes	No	No	No
Seizures	Yes	No	No	No	Yes	Yes	No	n.a.	n.a.
Oculomotor abnormalities	n.a.	Yes	Yes	No	Yes	Yes	No	n.a.	n.a.
Brain MRI (age at examination)	Leigh syndrome, bilateral frontal white matter hypo-attenuation, MRS: lactate peak in multiple areas (n.a.)	Cerebellar atrophy, T2 hyperintensities in the medulla oblongata (21 y)	Agenesis of the CC, abnormal cortical gyration, periventricular leukomalacia (n.a.)	Normal (17 y)	CC hypoplasia, cerebral atrophy predominantly of the frontal lobes, global delay of myelination (4 y)	Global cerebral atrophy, abnormal frontal lobe gyration, reduced white matter volume (18 m)	Normal (17 y)	n.d.	Normal (13 y)
Spinal MRI (age at examination)	n.d.	n.d.	n.a.	Normal (17 y)	n.a.	n.a.	Normal (17 y)	n.a.	n.a.
Muscle RC complex / blood / CSF lactate	n.a. / n.a. / n.a.	Normal / Normal / n.d.	n.a. / Normal / n.d.	n.d. / n.d. / n.a.	n.a. / Normal / Normal	Normal / Normal / Normal	n.d. / n.d. / n.d.	n.d. / n.d. / n.d.	n.d. / n.d. / n.d.
Blood tyrosine / urine organic acids	n.a. / n.a.	Normal / Normal 4-HPP, 4-HPL and 4-HPA	Normal / Normal[1]	Normal / n.a.	Normal / Normal[1]	Normal / Normal[1]	n.d. / n.d.	n.d. / n.d.	n.d. / n.d.

(continued on next page)

Supplementary Table 3 Clinical, neuroimaging and laboratory findings in individuals with biallelic *HPDL* variants (continued from previous page)

Family	TUE	ZA	ZB		ZC	ZD		ZE
Country of origin / Consanguinity	Syria / Yes	Japan / No	Pakistan / Yes		Czech Republic / No	China / No		Iran / Yes
***HPDL* cDNA variant(s)**	c.149G>A (hom.)	c.493A>C (hom.)	c.3G>C (hom.)		c.816_817del / c.523_529del	c.995del / c.650T>C		c.679del (hom.)
HPDL protein variant(s)	p.Gly50Asp (hom.)	p.Thr165Pro (hom.)	p.Met1? (hom.)		p.Val273fs / p.Thr175fs	p.Thr332fs / p.Leu217Pro		p.Thr227fs (hom.)
Individual	TUE1	ZA1	ZB1	ZB2	ZC1	ZD1	ZD2	ZE1
Sex / age at diagnosis / age at examination	M / 12 y / 15 y	M / 6 y / 15 y	M / 7 m / 19 m	M / 4 m / 6 y	F / 7 y / 12 y	M / 1 m / 5 y	F / 6 m / 6 m (died at age 8 m)	F / 7 y / 15 y
First symptom(s)	LL stiffness and pain	Abnormal gait	Lethargy, re-current vomiting, myoclonic jerks	Lethargy, myoclonic jerks	Abnormal gait	Increased muscle tone in LL	Infantile spasms, GDD	Abnormal gait
Disease severity / course	Mild / slowly progressive	Intermediate / progressive	Severe / episodic deteriorations	Severe / episodic deteriorations	Intermediate / progressive	Severe / non-progressive	Severe / episodic deteriorations	Intermediate / progressive
Motor delay / best motor ability reached	No / walking	Yes / walking	Yes / head control	Yes / sitting, crawling	No / walking	Yes / crawling	Yes / n.a.	No / walking
Cognitive delay	No	No	Yes	Yes	No	Yes	Yes	No
Spastic gait	Yes	n.e. (wheelchair)	n.e. (no walking)	n.e. (no walking)	Yes	n.e. (no walking)	n.e. (too young)	Yes
UL pyramidal signs / spasticity / weakness	No / No / No	Yes / No / No	Yes / Yes / Yes	Yes / Yes / Yes	No / No / No	Yes / Yes / Yes	Yes / Yes / n.a.	Yes / Yes / No
LL pyramidal signs / spasticity / weakness	Yes / Yes / Yes	Yes / Yes / Yes	Yes / Yes / Yes	Yes / Yes / Yes	Yes / Yes / Yes	Yes / Yes / Yes	Yes / Yes / n.a.	Yes / Yes / Yes
Pseudobulbar signs	No	No	No	No	No	Yes	Yes	No
Bladder dysfunction	No	No	n.e. (too young)	Yes	No	n.a.	n.e. (too young)	Yes
Ataxia	No	No	No	No	Yes	Yes	Yes	No
Encephalopathic episodes	No	No	Yes	Yes	No	No	Yes (causing death)	No
Contractures	Yes	Yes	Yes	Yes	Yes	Yes	No	Yes
Seizures	No	No	Yes	Yes	No	No	Yes	No
Oculomotor abnormalities	Yes	No	No	No	Yes	No	No	Yes
Brain MRI (age at examination)	Normal (13 y)	T2 hyperintensities in the right middle cerebellar peduncle and bilaterally in the medulla oblongata (15 y)	CC agenesis, global cerebral atrophy and ventriculomegaly, simplified gyral pattern, reduced white matter volume (19 m)	CC hypoplasia, global cerebral atrophy, simplified gyral pattern, reduced white matter volume (6 y)	Cerebellar atrophy, symmetric T2 hyperintensities in the medulla oblongata (12 y)	CC hypolplasia, generalized reduction of cerebral white matter volume (5 y)	n.a.	Dysplastic CC, cerebellar atrophy, symmetric T2 hyperintensities in the medulla oblongata (8 y)
Spinal MRI (age at examination)	Normal (14 y)	Normal (15 y)	Normal (19 m)	n.d.	Normal (12 y)	n.a.	n.a.	Normal (8 y)
Muscle RC complex / blood / CSF lactate	n.d. / n.d. / n.d.	n.d. / Normal / Normal	n.a. / n.a. / n.a.	n.a. / n.a. / n.a.	n.a. / Normal / Normal	n.a. / n.a. / n.a.	n.a. / n.a. / n.a.	n.a. / Normal / n.a.
Blood tyrosine / urine organic acids	n.d. / n.d.	n.d. / n.d.	Normal / Normal[1]	Normal / Normal[1]	Normal / Normal[1]	Normal / n.a.	n.a. / n.a.	n.a. / Normal[1]

(continued on next page)

Supplementary Table 3 Clinical, neuroimaging and laboratory findings in individuals with biallelic *HPDL* variants (continued from previous page)

Family	ZF	ZG	ZH			ZI	ZJ	ZK
Country of origin / Consanguinity	Ireland / No	UK / No	Italy / Yes			Pakistan / Yes	Saudi Arabia / No	Iran / Yes
HPDL cDNA variant(s)	c.232G>A / c.835C>T	c.692C>G / c.529_530del	c.1072T>G (hom.)			c.110G>C (hom.)	c.788C>G (hom.)	c.256del (hom.)
HPDL protein variant(s)	p.Ala78Thr / p.Gln279*	p.Ala231Gly / p.Leu177fs	p.Trp358Gly (hom.)			p.Arg37Pro (hom.)	p.Thr263Arg (hom.)	p.Ala86fs (hom.)
Individual	ZF1	ZG1	ZH1	ZH2	ZH3	ZI1	ZJ1	ZK1
Sex / age at diagnosis / age at examination	M / 8 y / 8 y	M / 12 y / 12 y	F / infancy / 7 y	M / 3 m / 3 y	M / infancy / 3 y	F / 11 m / 3.5 y	M / infancy / n.a.	F / 12 m / 11 y
First symptom(s)	Abnormal gait, frequent falls	Abnormal gait	Infantile spasms, hypsarrhythmia	Infantile spasms, hypsarrhythmia	Infantile spasms, hypsarrhythmia	Motor delay (inability to sit)	GDD	Motor delay
Disease severity / course	Mild / n.e.	Mild / n.e.	Severe / non-progressive	Severe / non-progressive	Severe / non-progressive	Severe / non-progressive	Severe / non-progressive	Severe / non-progressive
Motor delay / best motor ability reached	No / walking	No / walking	Yes / n.a.	Yes / n.a.	Yes / n.a.	Yes / standing with support	Yes / n.a.	Yes / crawling
Cognitive delay	No	No	Yes	Yes	Yes	Yes	Yes	Yes
Spastic gait	Yes	Yes	n.a.	n.e. (no walking)	n.e. (no walking)	n.e. (no walking)	n.a.	n.e. (no walking)
UL pyramidal signs / spasticity / weakness	n.a. / No / No	n.a. / No / No	Yes / Yes / Yes	Yes / Yes / Yes	Yes / Yes / Yes	Yes / Yes / Yes	Yes / Yes /Yes	n.a. / Yes / n.a.
LL pyramidal signs / spasticity / weakness	Yes / Yes / Yes	Yes / Yes / Yes	Yes / Yes / Yes	Yes / Yes / Yes	Yes / Yes / Yes	Yes / Yes / Yes	Yes / Yes /Yes	Yes / Yes / Yes
Pseudobulbar signs	n.a.	No	Yes	n.a.	Yes	No	n.a.	Yes
Bladder dysfunction	n.a.	No	n.a.	n.e. (too young)	n.e. (too young)	n.e. (too young)	n.a.	Yes
Ataxia	No	No	No	No	No	No	n.a.	No
Encephalopathic episodes	No	No	No	No	No	No	No	No
Contractures	No	No	No	No	No	Yes	Yes	Yes
Seizures	No	No	Yes	Yes	Yes	No	Yes	No
Oculomotor abnormalities	No	No	No	No	No	No	No	No
Brain MRI (age at examination)	Normal (8 y)	n.a.	CC hypoplasia, hypomyelination particularly of the corticospinal tract (n.a.)	CC hypoplasia, hypomyelination particularly of the corticospinal tract (n.a.)	CC hypoplasia, hypomyelination particularly of the corticospinal tract (n.a.)	CC hypoplasia (3.5 y)	CC agenesis, global cerebral atrophy and ventriculomegaly (n.a.)	CC agenesis, widening of occipital horns of lateral ventricles (n.a.)
Spinal MRI (age at examination)	Normal (8 y)	n.a.	n.d.	n.d.	n.d.	Normal (3.5 y)	n.d.	n.d.
Muscle RC complex / blood / CSF lactate	n.a. / Normal / n.a.	n.a. / n.a. / n.a.	n.d. / n.a. / n.a.	n.d. / n.a. / n.a.	n.d./ n.a. / n.a.	n.d. / n.d. / n.d.	n.d. / n.d. / n.d.	n.d. / n.d. / n.d.
Blood tyrosine / urine organic acids	Normal / n.a.	n.a. / n.a.	Normal / Normal[1]	Normal / Normal[1]	Normal / Normal[1]	n.d. /n.d.	n.d. / n.d.	n.d. / n.d.

[1]Reports on urine organic acids profile did not explicitly refer to 4-HPP, 4-HPL and 4-HPA.
ADEM = acute disseminated encephalomyelitis; CC = corpus callosum; CSF = cerebrospinal fluid; d = day(s); F = female; GDD = global developmental delay; hom. = homozygous; LL = lower limbs; M = male; m = month(s); MRI = magnetic resonance imaging; MRS = magnetic resonance spectroscopy; n.a. = not available; n.d. = not determined; n.e. = not examinable (e.g., child too young to assess walking ability); RC = respiratory chain; UL = upper limbs; y = year(s).

Supplementary Table 4 Conservation scores of HPDL residues affected by missense variants

	GERP++ score[1]	PhastCons100way score[2]	PhyloP100way score[2]
c.110G>C (p.Arg37Pro)	5.06	1.000	7.930
c.149G>A (p.Gly50Asp)	4.93	1.000	5.968
c.232G>A (p.Ala78Thr)	4.93	1.000	8.275
c.418G>A (p.Gly140Arg)	5.04	1.000	8.769
c.493A>C (p.Thr165Pro)	5.11	1.000	4.314
c.503G>A (p.Cys168Tyr)	5.11	1.000	6.902
c.518C>A (p.Ser173Tyr)	5.11	0.997	5.009
c.569C>T (p.Pro190Leu)	5.11	0.982	3.285
c.650T>C (p.Leu217Pro)	5.31	1.000	4.932
c.692C>G (p.Ala231Gly)	5.31	0.983	2.605
c.788C>G (p.Thr263Arg)	5.14	1.000	7.086
c.788C>T (p.Thr263Met)	5.14	1.000	7.086
c.797T>C (p.Ile266Thr)	5.14	1.000	7.185
c.847C>T (p.Pro283Ser)	5.14	0.998	3.392
c.859T>C (p.Tyr287His)	5.14	1.000	7.185
c.1013T>C (p.Leu338Pro)	5.14	1.000	7.185
c.1072T>G (p.Trp358Gly)	4.47	1.000	5.606

[1]GERP++ (Davydov *et al.*, 2010) estimates evolutionary constraint of specific positions in 36 mammalian species. Scores range from -12.36 to 6.18 with higher scores indicating more conserved sites.
[2]PhastCons and PhyloP (Pollard *et al.*, 2010) conservation scores are based on multiple alignments of 100 vertebrate genomes. Scores range from 0 to 1 for PhastCons and from -20 to 9.87 for PhyloP with higher scores suggesting stronger conservation of the site.

Supplementary Table 5 Allele counts and frequencies of *HPDL* variants in public databases

	GnomAD_all exomes[1]		ESP[2]		1000G[3]	
	AC	AF	AC	AF	AC	AF
c.3G>C (p.Met1?)	6	2.962e-05	0	0	0	0
c.27C>A (p.Cys9*)	0	0	0	0	0	0
c.110G>C (p.Arg37Pro)	1	4.367e-06	0	0	0	0
c.149G>A (p.Gly50Asp)	2	1.018e-05	0	0	0	0
c.232G>A (p.Ala78Thr)	0	0	0	0	0	0
c.256del (p.Ala86fs)	1	4.896e-06	0	0	0	0
c.342_345dup (p.Ala116fs)	0	0	0	0	0	0
c.418G>A (p.Gly140Arg)	0	0	0	0	0	0
c.493A>C (p.Thr165Pro)	1	4.124e-06	0	0	0	0
c.503G>A (p.Cys168Tyr)	2	8.246e-06	0	0	0	0
c.518C>A (p.Ser173Tyr)	0	0	0	0	0	0
c.523_529del (p.Thr175fs)	0	0	0	0	0	0
c.529_530del (p.Leu177fs)	0	0	0	0	0	0
c.569C>T (p.Pro190Leu)	1	4.042e-06	1	1.539e-04	0	0
c.650T>C (p.Leu217Pro)	0	0	0	0	0	0
c.679del (p.Thr227fs)	0	0	0	0	0	0
c.692C>G (p.Ala231Gly)	0	0	0	0	0	0
c.769_771delinsTC (p.Gln257fs)	0	0	0	0	0	0
c.788C>G (p.Thr263Arg)	0	0	1	1.539e-04	0	0
c.788C>T (p.Thr263Met)	3	1.306e-05	0	0	1	1.997e-04
c.797T>C (p.Ile266Thr)	2	8.506e-06	0	0	0	0
c.816_817del (p.Val273fs)	0	0	0	0	0	0
c.835C>T (p.Gln279*)	2	8.032e-06	0	0	0	0
c.847C>T (p.Pro283Ser)	12	4.793e-05	0	0	0	0
c.859T>C (p.Tyr287His)	25	9.954e-05	0	0	0	0
c.995del (p.Thr332fs)	1	3.977e-06	0	0	0	0
c.1013T>C (p.Leu338Pro)	6	2.387e-05	4	6.154e-04	0	0
c.1072T>G (p.Trp358Gly)	6	2.962e-05	0	0	0	0

[1]GnomAD_all exomes: 123,136 exomes from unrelated individuals sequenced as part of various disease-specific and population genetic studies contained in the Genome Aggregation Database (gnomAD) (Lek *et al.*, 2016).

[2]ESP: Exomes from 6,503 individuals with heart, lung and blood disorders included in the NHLBI GO Exome Sequencing Project (ESP) (Fu *et al.*, 2013).

[3]1000G: Genomes from 2,504 individuals who declared themselves to be healthy at the time the samples were collected (Sudmant *et al.*, 2015).

AC = allele counts, AF = allele frequencies

Supplementary Table 6 *In silico* predictions of the effects of *HPDL* missense variants

	CADD prediction (phred-like score)[1]	PolyPhen-2 prediction (score)[2]	MutationAssessor prediction (score)[3]	LRT prediction (LRT$_{new}$ score)[4]	MutationTaster2 prediction (score)[5]
c.110G>C (p.Arg37Pro)	Damaging (26.4)	Possibly damaging (0.491)	Medium (2.81)	Deleterious (1.000)	Disease causing (0.999)
c.149G>A (p.Gly50Asp)	Damaging (24.7)	Probably damaging (0.931)	Medium (2.81)	Deleterious (0.999)	Disease causing (0.999)
c.232G>A (p.Ala78Thr)	Damaging (26.4)	Probably damaging (0.925)	Medium (2.60)	Deleterious (0.999)	Disease causing (0.999)
c.418G>A (p.Gly140Arg)	Damaging (28.0)	Possibly damaging (0.706)	Medium (2.91)	Deleterious (0.999)	Disease causing (0.999)
c.493A>C (p.Thr165Pro)	Damaging (28.7)	Probably damaging (0.953)	Medium (2.98)	Deleterious (0.999)	Disease causing (0.996)
c.503G>A (p.Cys168Tyr)	Damaging (29.8)	Probably damaging (0.984)	Medium (3.07)	Deleterious (0.999)	Disease causing (1.000)
c.518C>A (p.Ser173Tyr)	Damaging (22.9)	Probably damaging (0.964)	Medium (2.84)	Deleterious (0.999)	Disease causing (0.992)
c.569C>T (p.Pro190Leu)	Damaging (21.5)	Benign (0.010)	Medium (1.94)	Deleterious (0.999)	Disease causing (1.000)
c.650T>C (p.Leu217Pro)	Damaging (25.8)	Probably damaging (0.983)	Medium (2.77)	Deleterious (0.974)	Disease causing (1.000)
c.692C>G (p.Ala231Gly)	Damaging (23.3)	Possibly damaging (0.703)	Medium (3.02)	Deleterious (0.999)	Disease causing (0.999)
c.788C>G (p.Thr263Arg)	Damaging (24.5)	Probably damaging (0.999)	Medium (3.33)	Deleterious (1.000)	Disease causing (1.000)
c.788C>T (p.Thr263Met)	Damaging (24.7)	Probably damaging (0.998)	Medium (3.33)	Deleterious (1.000)	Disease causing (1.000)
c.797T>C (p.Ile266Thr)	Damaging (23.6)	Probably damaging (0.998)	Medium (3.39)	Deleterious (0.999)	Disease causing (1.000)
c.847C>T (p.Pro283Ser)	Damaging (23.0)	Probably damaging (0.944)	Medium (3.07)	Deleterious (0.999)	Disease causing (0.996)
c.859T>C (p.Tyr287His)	Damaging (26.2)	Probably damaging (1.000)	Medium (3.31)	Deleterious (1.000)	Disease causing (0.999)
c.1013T>C (p.Leu338Pro)	Damaging (31.0)	Probably damaging (0.993)	Medium (3.22)	Deleterious (0,999)	Disease causing (1.000)
c.1072T>G (p.Trp358Gly)	Damaging (33.0)	Probably damaging (0.972)	Medium (2.69)	Deleterious (1.000)	Disease causing (0.999)

[1]CADD (Kircher *et al.*, 2014) phred-like rank scores above 15 (for a more conservative estimate: above 20) are considered "damaging".

[2]PolyPhen-2 (Adzhubei *et al.*, 2010) scores near 1 are most strongly predicting a "damaging" effect of an amino substitution.

[3]MutationAssessor (Reva *et al.*, 2011) scores range from -5.14 to 6.49 with higher scores indicating increasing likelihood of functional impact of a variant. Score cutoff between "neutral", "low", "medium" and "high" predictions are 0.8, 1.94 and 3.50.

[4]Values for the LRTnew (Chun & Fay, 2009) score range from 0 to 1 with higher values indicating a variant is more likely to be "deleterious".

[5]The probability value given by MutationTaster2 (Schwarz *et al.*, 2010) is the probability of the prediction, i.e. a value close to 1 indicates a high "security" of the prediction.

Supplementary Table 7 *In silico* prediction of HPDL's putative mitochondrial localization

Algorithm	Score	Prediction
MitoProt[1]	0.97	mitochondrial
iPSORT[2]	1.0	mitochondrial
IMPI[3]	0.99	mitochondrial

[1]For Mitoprot, a score close to 1 suggests mitochondrial localization (Claros & Vincens, 1996).
[2]For iPSORT, a score close to 1 supports mitochondrial localization (Bannai *et al.*, 2002).
[3]Prediction from the Integrated Mitochondrial Protein Index (IMPI) gene database. A score close to 1 supports mitochondrial localization (Smith & Robinson, 2019).

Supplementary Table 8 *In silico* predictions of HPDL's putative transmembrane domain

Algorithm	Score	Prediction
TMpred[1]	1,184	TM at residues 115-133
MEMSAT[2]	n.a.	TM at residues 114-133
PRED-TMR[3]	n.a.	TM at residues 114-133

[1]TMpred makes a prediction of membrane-spanning regions and their orientation. Scores >500 are considered significant (Hofmann & Stoffel, 1993).
[2]MEMSAT is a method capable of automatically identifying pore-lining regions from sequence information alone (Jones *et al.*, 1994).
[3]PRED-TMR refines a standard hydrophobicity analysis with a detection of potential termini of transmembrane regions (Pasquier *et al.*, 1999).
n.a. = not available; TM = transmembrane domain

Supplementary References

Adzhubei IA, Schmidt S, Peshkin L, Ramensky VE, Gerasimova A, Bork P, Kondrashov AS, Sunyaev SR (2010) A method and server for predicting damaging missense mutations. *Nat Methods* 7: 248-249

Bannai H, Tamada Y, Maruyama O, Nakai K, Miyano S (2002) Extensive feature detection of N-terminal protein sorting signals. *Bioinformatics* 18: 298-305

Chun S, Fay JC (2009) Identification of deleterious mutations within three human genomes. *Genome Res* 19: 1553-61

Claros MG, Vincens P (1996) Computational method to predict mitochondrially imported proteins and their targeting sequences. *Eur J Biochem* 241: 779-86

Davydov EV, Goode DL, Sirota M, Cooper GM, Sidow A, Batzoglou S (2010) Identifying a high fraction of the human genome to be under selective constraint using GERP++. *PLoS Comput Biol* 6: e1001025

Fu W, O'Connor TD, Jun G, Kang HM, Abecasis G, Leal SM, Gabriel S, Rieder MJ, Altshuler D, Shendure J, Nickerson DA, Bamshad MJ, Akey JM (2013) Analysis of 6,515 exomes reveals the recent origin of most human protein-coding variants. *Nature* 493: 216-20

GTEx Consortium G (2013) The Genotype-Tissue Expression (GTEx) project. *Nat Genet* 45: 580-5

Hofmann K, Stoffel W (1993) TMbase-a database of membrane spanning proteins segments. *Biol Chem Hoppe Seyler* 347: 166

Jones DT, Taylor WR, Thornton JM (1994) A model recognition approach to the prediction of all-helical membrane protein structure and topology. *Biochemistry* 33: 3038-49

Kircher M, Witten DM, Jain P, O'Roak BJ, Cooper GM, Shendure J (2014) A general framework for estimating the relative pathogenicity of human genetic variants. *Nat Genet* 46: 310-5

Larkin MA, Blackshields G, Brown NP, Chenna R, McGettigan PA, McWilliam H, Valentin F, Wallace IM, Wilm A, Lopez R, Thompson JD, Gibson TJ, Higgins DG (2007) Clustal W and Clustal X version 2.0. *Bioinformatics* 23: 2947-8

Lek M, Karczewski KJ, Minikel EV, Samocha KE, Banks E, Fennell T, O'Donnell-Luria AH, Ware JS, Hill AJ, Cummings BB, Tukiainen T, Birnbaum DP, Kosmicki JA, Duncan LE, Estrada K, Zhao F, Zou J, Pierce-Hoffman E, Berghout J, Cooper DN et al. (2016) Analysis of protein-coding genetic variation in 60,706 humans. *Nature* 536: 285-91

Niemann A, Ruegg M, La Padula V, Schenone A, Suter U (2005) Ganglioside-induced differentiation associated protein 1 is a regulator of the mitochondrial network: new implications for Charcot-Marie-Tooth disease. *J Cell Biol* 170: 1067-78

Pasquier C, Promponas VJ, Palaios GA, Hamodrakas JS, Hamodrakas SJ (1999) A novel method for predicting transmembrane segments in proteins based on a statistical analysis of the SwissProt database: the PRED-TMR algorithm. *Protein Eng* 12: 381-5

Pollard KS, Hubisz MJ, Rosenbloom KR, Siepel A (2010) Detection of nonneutral substitution rates on mammalian phylogenies. *Genome Res* 20: 110-21

Reva B, Antipin Y, Sander C (2011) Predicting the functional impact of protein mutations: application to cancer genomics. *Nucleic Acids Res* 39: e118

Schwarz JM, Rodelsperger C, Schuelke M, Seelow D (2010) MutationTaster evaluates disease-causing potential of sequence alterations. *Nat Methods* 7: 575-6

Smith AC, Robinson AJ (2019) MitoMiner v4.0: an updated database of mitochondrial localization evidence, phenotypes and diseases. *Nucleic Acids Res* 47: D1225-D1228

Sudmant PH, Rausch T, Gardner EJ, Handsaker RE, Abyzov A, Huddleston J, Zhang Y, Ye K, Jun G, Hsi-Yang Fritz M, Konkel MK, Malhotra A, Stutz AM, Shi X, Paolo Casale F, Chen J, Hormozdiari F, Dayama G, Chen K, Malig M et al. (2015) An integrated map of structural variation in 2,504 human genomes. *Nature* 526: 75-81